AD_____

Award Number: W81XWH-04-1-0493

TITLE: Functional Analysis of the Beclin-1 Tumor Suppressor Interaction with hVps34 (Type III PI3'-kinase) in Breast Cancer Cells

PRINCIPAL INVESTIGATOR: William A. Maltese, Ph.D.

CONTRACTING ORGANIZATION: Medical College of Ohio
Toledo, OH 43614

REPORT DATE: June 2005

TYPE OF REPORT: Annual

PREPARED FOR: U.S. Army Medical Research and Materiel Command
Fort Detrick, Maryland 21702-5012

REPORT DOCUMENTATION PAGE

Form Approved
OMB No. 074-0188

1. AGENCY USE ONLY	2. REPORT DATE	3. REPORT TYPE AND DATES COVERED
	June 2005	Annual (7 May 2004 - 6 May 2005)

4. TITLE AND SUBTITLE
Functional Analysis of the Beclin-1 Tumor Suppressor Interaction with hVps34 (Type III PI3'-kinase) in Breast Cancer Cells

5. FUNDING NUMBERS
W81XWH-04-1-0493

6. AUTHOR(S)
William A. Maltese, Ph.D.

7. PERFORMING ORGANIZATION NAME(S) AND ADDRESS(ES)
Medical College of Ohio
Toledo, OH 43614

E-Mail: wmaltese@mco.edu

8. PERFORMING ORGANIZATION REPORT NUMBER

9. SPONSORING / MONITORING AGENCY NAME(S) AND ADDRESS(ES)
U.S. Army Medical Research and Materiel Command
Fort Detrick, Maryland 21702-5012

10. SPONSORING / MONITORING AGENCY REPORT NUMBER

11. SUPPLEMENTARY NOTES
Original contains color plates: ALL DTIC reproductions will be in black and white

12a. DISTRIBUTION / AVAILABILITY STATEMENT
Approved for Public Release; Distribution Unlimited

12b. DISTRIBUTION CODE

13. ABSTRACT (Maximum 200 Words)

Macroautophagy plays a pivotal role in type II programmed cell death. This form of cell death entails early accumulation of autophagic vacuoles. Beclin 1 has been implicated in the regulation of macroautophagy. Previous reports indicate that overexpression of Beclin can promote autophagy and inhibit tumorigenesis in cultured breast carcinoma cells, and conversely, that heterozygous disruption of the Beclin gene can promote tumorigenesis in mice. During the first year we have performed immunoprecipitation studies with MCF7 breast carcinoma and U251 glioma cells, and found that Beclin associates with the human class III phosphatidylinositol 3-kinase (PI3K), hVps34, but not with another putative partner, Bcl-2. The lipid product of Vps34, PI(3)P, is required not only for autophagy, but also for assembly of proteins involved in endocytosis and trafficking of enzymes from the trans-Golgi network to the lysosomes. Therefore we set out to determine if the apparent tumor suppressing activity of Beclin is directly related to its role in autophagy, or is instead related to a role in controlling endocytic trafficking of growth factors or cellular nutrients. Retroviral RNAi-mediated gene silencing was initially used to suppress Beclin expression in MCF7 breast carcinoma cells. In these cells, Beclin knockdown (KD) was incomplete (65%). Therefore, we turned to the U-251cell line, which is more easily infected with retroviral vectors. In these a cells a 95% KD of Beclin was achieved, allowing definitive studies of autophagy and protein trafficking. The results of these studies indicate that Beclin is required for hVps34 to function in autophagy, but is dispensable for hVps34 to function in the trafficking of the lysosomal enzymes or endocytosis of growth factor receptors or fluid phase markers. Beclin and hVps34 appear to exist in a high molecular weight complex in several cell lines including MCF7. Therefore, we are currently using FLAG-tagged Beclin in stable MCF7 cell lines to isolate and identify the components of this complex by mass spectrometry.

14. SUBJECT TERMS
Breast Cancer

15. NUMBER OF PAGES
99

16. PRICE CODE

17. SECURITY CLASSIFICATION OF REPORT	18. SECURITY CLASSIFICATION OF THIS PAGE	19. SECURITY CLASSIFICATION OF ABSTRACT	20. LIMITATION OF ABSTRACT
Unclassified	Unclassified	Unclassified	Unlimited

Table of Contents

Introduction

The general goal of this study is to define at the molecular level the basis for the tumor suppressor function of Beclin-1 in breast cancer. We hypothesize that the primary intracellular partner for Beclin in human cells is a class-III phosphatidylinositol 3'-kinase termed hVps34 [1]. We further hypothesize that Beclin is essential for engaging hVps34 in macroautophagy, but is not required for the other functions of hVps34 in protein trafficking [2-4]. Macroautophagy is a process whereby cytoplasmic proteins and organelles are incorporated into vacuoles termed autophagosomes, and subsequently are degraded when these structures fuse with lysosomes [5;6]. Some types of cells use macroautophagy as a short-term survival strategy in response to stress or nutrient deprivation. However, autophagy is also a diagnostic feature of type-II programmed cell death (distinct from apoptosis) [7], which is known to occur during the regression of hormone-dependent breast cancer cells treated with tamoxifen and related compounds [8;9]. By understanding how Beclin regulates macroautophagy, it might be possible to manipulate this process to stimulate type-II cell death in malignant cells. We are using siRNA-mediated gene silencing to deplete Beclin in cultured cells and determine whether or not Beclin selectively affects the function of hVps34 in autophagy versus normal trafficking. We have also observed that Beclin and hVps34 coexist in a high molecular weight cytoplasmic complex, suggesting the presence of other unidentified protein components. To define the components of the Beclin/hVps34 protein complex, we have developed stable breast cancer cell line that expresses FLAG-tagged Beclin, and we have begun to isolate the Beclin complexes on anti-FLAG affinity beads. The protein complexes will be defined by mass spectrometry to identify additional proteins besides Beclin and hVps34. Once we know the components of the Beclin complex, we will begin to test the consequences of their depletion for regulation of cell growth and death pathways in experiments with tamoxifen-treated breast cancer cell lines.

Body

This progress report will follow the outline of the Objectives listed in the Statement of Work described in the original grant proposal. For each objective I will indicate what has been done, what is planned for the next year, and where we may wish to adopt a modified research strategy.

Objective 1: Test the hypothesis that Beclin-1 acts through Vps34 to mediate autophagic cell death in cultured breast carcinoma cells.

Task 1. Suppression of Beclin-1 expression in MCF7 cells by siRNA-mediated gene silencing and evaluation of the effects of this manipulation on the development of autophagosomes and autophagic cell death in response to tamoxifen or nutritional deprivation.

Progress: We have attempted to suppress Beclin expression using pSuper retroviral constructs in MCF7 breast carcinoma cells according to the original plan. Based on western blot analysis, we have achieved a 65% suppression of Beclin expression. However the residual level of Beclin is too high to permit a definitive analysis of the effects of Beclin depletion on autophagy and protein trafficking. An example of the effects of siRNA–mediated Beclin silencing in MCF7 cells is shown in Fig. 1A. To circumvent the problem of high residual Beclin expression, we turned to a different cell line that exhibits high infection efficiency with the retroviral vector (*e.g.,* the U-251 glioblastoma cell line). As shown in Fig. 1B, we were able to obtain a 95% suppression of Beclin expression in this cell line. Although U-251 is not a breast tumor line, our immunoprecipitation studies have indicated that hVps34 is a major Beclin partner in these cells (Fig 2B), just as it is in MCF7 cells (Fig. 2A). Therefore, because we were able to obtain a near-complete knockdown of Beclin in the U-251 cell line, we opted to use it for basic cell biological studies to assess the importance of Beclin for hVps34 function. To provide a point of reference for the manipulations of Beclin expression, we also utilized siRNA to suppress the expression of Vps34 itself in the U-251 cells. Detailed characterization of the effects of

Vps34 depletion identified a specific role for this PI 3-kinase in the late endosome compartment, but not the early endosomes.

Fig. 1. siRNA-mediated silencing of Beclin expression in MCF7 breast carcinoma and U-251 glioblastoma cells

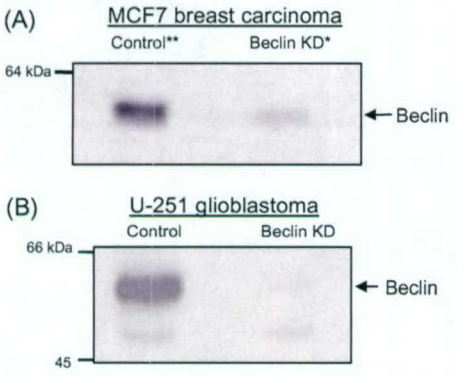

* A short hairpin RNA was designed to target a 19 bp sequence specific to Beclin mRNA. ** A control vector was constructed with an insert that would not target any sequence in the human genome. Cells were infected with pSUPER retrovirus and selected in medium containing 1 μg/ml puromycin for 7 days to generate stable cell lines.

Fig. 2. The endogenous Beclin complex immunoprecipitated from MCF7 breast carcinoma and U-251 glioblastoma cells contains hVps34 PI-3 Kinase

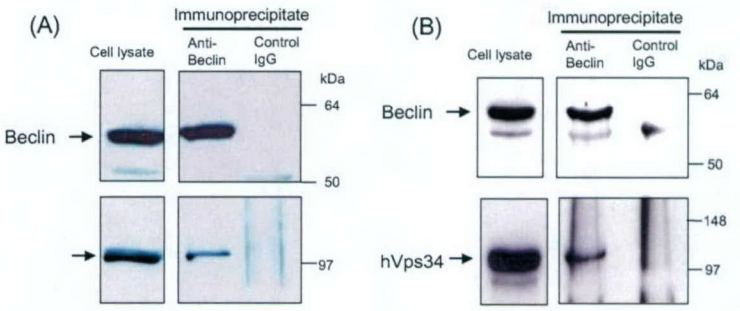

The results of these basic cell biological studies have been described in two separate manuscripts submitted for publication to the *Journal of Cell Science* (Beclin studies) and *Experimental Cell Research* (Vps34 studies). Copies of these manuscripts are attached as Appendices. Both manuscripts have been returned to us for revisions and we anticipate that they will be accepted once the revisions are completed. The major conclusions reported in Beclin the manuscript are 1) that knockdown of Beclin expression by siRNA-mediated gene silencing interferes with the initiation of macroautophagy, a process that depends on hVps34, and 2) that depletion of Beclin has little or no effect on endocytic and lysosomal trafficking steps reported to depend on hVps34. The results suggest that Beclin functions selectively to target or activate hVps34 in the autophagy pathway, but not the normal protein trafficking pathways.

Task 2. Over-expression of wild-type Beclin or Vps34-interaction-deficient Beclin (Δ80-107) and evaluation of the effects of this manipulation on the development of autophagosomes in other estrogen receptor positive (T47D, ZR-75) and negative (MDA-MB231) breast cancer cell lines.

Progress: We have generated stable MCF7 breast cancer cell lines that over-express FLAG-tagged wild-type Beclin and Beclin (Δ80-107) under control of a tetracycline-responsive promoter (tet-off) (Fig. 3). The Δ80-107 Beclin mutant lacks a domain required for interaction with Vps34 (Fig. 4). During the coming year we plan to continue this task by evaluating the autophagic death response in these cells after exposure to tamoxifen.

Fig. 3 Inducible expression of FLAG-Beclin (wild-type or Δ80-107) in MCF7 Tet-off cells

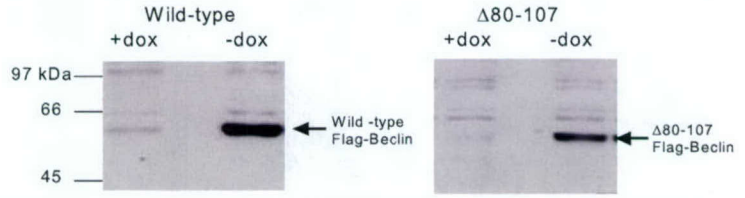

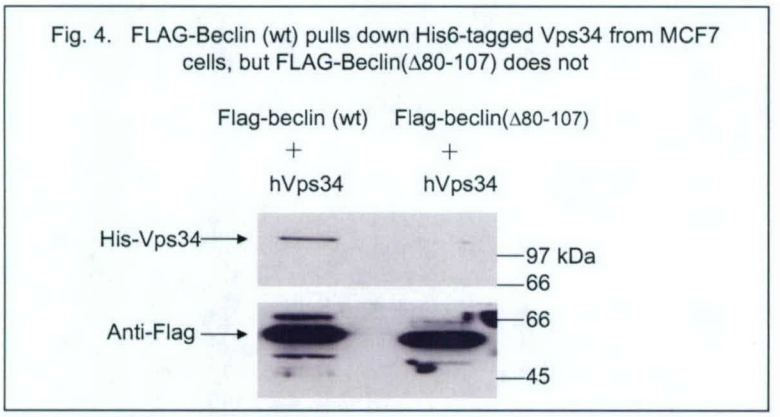

Fig. 4. FLAG-Beclin (wt) pulls down His6-tagged Vps34 from MCF7 cells, but FLAG-Beclin(Δ80-107) does not

Task 3. Examination of the effects of Beclin gene-silencing on autophagy in other estrogen receptor positive (T47D, ZR-75) and negative (MDA-MB231) breast cancer cell lines with higher (compared to MCF7) Beclin expression.

Progress: While the studies on the basic cell biology of Beclin in protein trafficking were being conducted with U-251 cells, we continued to experiment with siRNA-mediated suppression of Beclin in estrogen receptor-positive breast cancer cell lines other than MCF7, so that we could come back to the question of how Beclin depletion might affect the response of these cells to anti-estrogens. In T47D cells we were able to obtain a 60-65% suppression of Beclin expression similar to what we observed in MCF7. However, in ZR-75 cells the siRNA was much more effective, resulting in 90-95% knockdown of Beclin expression (Fig. 5). Thus, during the next year of the project we will determine how the loss of Beclin in these cells will affect the initiation of autophagy and cell death in response to tamoxifen.

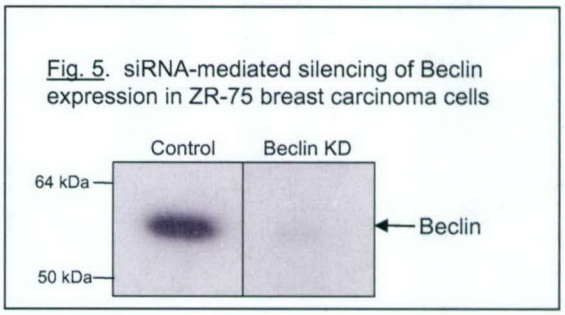

Fig. 5. siRNA-mediated silencing of Beclin expression in ZR-75 breast carcinoma cells

Objective 2. Define the mechanism of Beclin action by determining whether Beclin regulates the catalytic activity or membrane recruitment of hVps34 PI-3'-kinase.

Task 1. Studies of the effects of recombinant Beclin on the activity of hVps34 *in vitro*.

Progress: Efforts to produce sufficient quantities of recombinant Beclin in *E. coli* have been hampered by the tendency of this protein to form insoluble aggregates when overexpressed in bacterial systems. However, the answer to the question posed in this task has been partially answer by studies describe below under Task 2. Those studies show that depletion of Beclin in intact cells has no detectable effect on endosomal morphology or transport processes mediated by Vps34 PI 3-kinase, suggesting that Beclin is not a "generic" activator of Vps34 that required to maintain optimal activity of the kinase under normal conditions. Based on these findings, we believe that Beclin is more likely to function in the specific targeting of Vps34 to the isolation membrane of the nascent autophagosomes.

Task 2. Assess the effects of Beclin on the activity of hVps34 in cultured cells.

Progress: Now that we have been able to achieve > 90% knockdown of Beclin expression in ZR-75 breast cancer cells (see Fig. 5 above), we are preparing to determine how the depletion of Beclin will affect the activity and subcellular distribution of hVps34. Based on our studies with U-251 cells, we do not expect to

observe marked difference in the activity of Vps34, as measured by the formation of PI(3)P. However, it is possible that loss of hVps34 may affect the subcellular localization of the kinase to membrane compartments, particularly under conditions where autophagy is induced. Thus, for the coming year we plan to fractionate the control and Beclin knockdown ZR-75 cells to determine the subcellular distribution of Vps34 under normal culture conditions and under conditions where autophagy is induced by various methods (nutrient deprivation, exposure to C2-ceramide, or tamoxifen treatment).

Objective 3: Elucidation of the nature of the Beclin-Vps34 complex by determining whether the interaction between Beclin and hVps34 is direct or indirect (Tasks 1 & 2), and identifying other proteins that may be part of the complex (Tasks 3-5). In particular, we will test the hypothesis that interaction of Beclin with hVps34 is mediated by p150, a known Vps34 partner, or by novel bridging proteins similar to Apg14 in yeast.

Task 1. Complete studies of the physical interaction between recombinant Beclin and hVps34 in vitro.

Task 2. Assess the effects of recombinant p150 on the interaction between Beclin and hVps34.

Progress: Preliminary size exclusion chromatography analyses of the endogenous cytosolic complexes containing Beclin and Vps34 in MCF7 breast cancer cells (Fig. 6) and U-251 glioma cells (Fig. 7) indicate that the protein complexes migrates at a much larger size than predicted by the individual molecular masses of Beclin (60 kDa) and Vps34 (105 kDa). Immunoblot studies of these Beclin/Vps34 fractions have failed to detect p150, which appears to be exclusively localized in membranes. Thus, we believe that an analysis of the interaction of recombinant Beclin with Vps34 and/or p150 (Tasks 1 and 2) should be deferred until we have identified the other protein components that appear to be present in the endogenous Beclin complex.

Fig. 6. Beclin and Vps34 from MCF7 breast carcinoma cells co-elute as a high molecular mass complex (Superose-6 column)

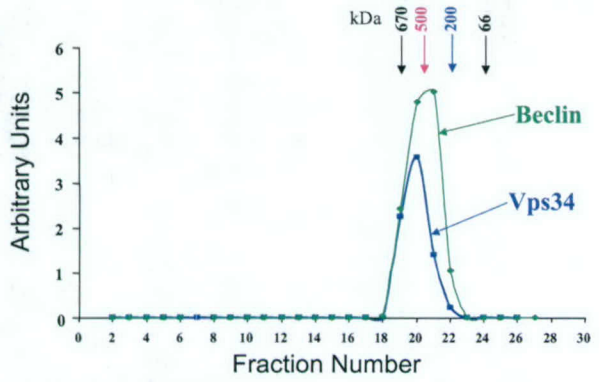

Fig. 7. Beclin and Vps34 from U-251 cells co-elute as a high molecular mass complex (Superose-12 column)

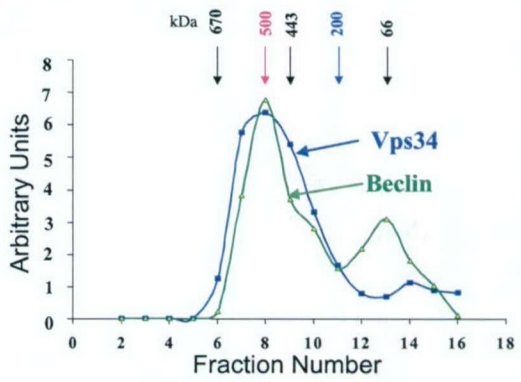

Task 3. Perform GST-Beclin interaction chromatography to identify other proteins that may be functional components of the Beclin/hVps34 complex.

Progress: We believe that identification of the other protein partners (besides Vps34) that exist in a complex with Beclin in human breast cancer cells should be the highest priority for the remainder of the project. Achieving this objective will be of central importance if we are to understand how Beclin specifically engages Vps34 in the autophagy pathway and ultimately affects the survival of the cells. Because we have been able to successfully generate a stable MCF7 breast cancer cell line that over-expresses FLAG-tagged Beclin (see Fig. 3), we propose a minor modification of the experimental approach. Instead of using recombinant GST-Beclin as an affinity ligand to capture cellular Beclin interacting proteins, we propose to perform FLAG-affinity pull-down assays to isolate the actual endogenous Beclin complex, followed by mass spectrometry to identify any unique protein components in the complex. This approach has a significant advantage over the use of

recombinant GST-Beclin since it avoids the potential pitfall of failing to isolating an endogenous interacting protein because it is already saturated with endogenous Beclin. We are currently performing pilot-scale FLAG pull-down studies to assess the feasibility of this approach.

Task 4. Perform yeast two-hybrid screen with Beclin as the bait to identify other proteins that may be functional components of the Beclin/hVps34 complex.

Progress: Because of the labor-intensive nature of the yeast two-hybrid approach and the high probability of obtaining false positives, we a planning to defer this task until we have thoroughly evaluated the FLAG-pull down + mass spec approach as a means to identify novel Beclin partners (Task 3).

Task 5. Begin to address the functional significance of any newly-identified Beclin interacting proteins for the formation of the Beclin-hVps34 complex and the initiation of autophagy in MCF7 cells. It is anticipated that this task will overlap with Tasks 3 & 4, as potentially important Beclin binding partners are identified by affinity chromatography and LC/MS/MS or yeast two-hybrid assay.

Progress: This task was originally planned for the final year of the project, after we have identified new Beclin interacting partners.

Key Research Accomplishments

1. Vps34 PI 3-kinase is an interacting partner for Beclin in human MCF7 and U-251 cells
2. Vps34 co-elutes with Beclin in a broad peak suggestive of a 500-600 kDa complex, indicating that there are other proteins in this complex besides these two proteins.
3. To study the role of Beclin in relation to the function of Vps34, we attempted to suppress the expression of Beclin in MCF7 breast carcinoma cells using siRNA. Although this approach was successful, the extent of Beclin suppression was incomplete. Similar problems were encountered with another breast cancer line (T47D)
4. To facilitate basic cellular studies of Beclin and Vps34, we turned to U-251 glioma cells, where we were able to obtain a much more extreme suppression of Beclin and/or Vps34 expression.
5. In U251-cells the apparent molecular mass of the cytosolic Vps34 complex is reduced to 200-300 kDa when Beclin expression is ablated in the Beclin knockdown cells. This suggests that Beclin is essential for the formation of the cytosolic Vps34 complex.
6. Beclin plays an essential role in Vps34-dependent macroautophagy induced by nutrient deprivation or treatment with C2-ceramide.
7. Knockdown of Vps34 expression demonstrates that this PI 3-kinase plays an important role in maintenance of late endosome morphology and trafficking of proteins to the lysosome.
8. However, Beclin is not required for Vps34 to function in lysosomal enzyme sorting and endocytic protein trafficking.
9. Therefore, Beclin's role as a tumor suppressor is most likely related to its specific role in regulating Vps34's function in macroautophagy.
10. A stable ZR-75 breast cancer cell line has been established with Beclin expression suppressed by more than 90%. This cell line will be used for future studies to determine whether Beclin plays a role in the induction of autophagic cell death in response to treatment with anti-estrogens.
11. Stable MCF7 breast cancer cell lines expressing FLAG-tagged wild-type and Vps34-binding-deficient forms of Beclin have been established. These will be used to isolate novel Beclin interacting partners that comprise the Vps34 complex.

Reportable Outcomes

Manuscripts Submitted:

Xuehuo Zeng, Jean H. Overmeyer and William A. Maltese (2005) Functional specificity of the mammalian Beclin-Vps34 PI 3-kinase complex in macroautophagy versus endocytosis and lysosomal enzyme sorting. *J. Cell Sci.* (in revision).

Erin E. Johnson, Jean H. Overmeyer, William T. Gunning and William A. Maltese (2005) Specific function of mammalian Vps34 phosphatidylinositol 3-kinase in late *versus* early endosomes revealed by siRNA-mediated gene silencing. *Exp. Cell Res.* (in revision)

Presentations:

Xuehuo Zeng and William A. Maltese (2004) Formation of a Beclin complex with Vps34 is required for autophagy but not endocytic trafficking. The American Society for Cell Biology 44th Annual Meeting, Washington, DC.

Johnson, E.E, Gunning, W.T., and Maltese W.A. (2004) Endosomal and lysosomal perturbations caused by siRNA-mediated silencing of Vps34 PI 3'-kinase expression in glioblastoma cells. The American Society for Cell Biology 44th Annual Meeting, Washington, DC.

Johnson, E.E., Gunning, W.T., and Maltese, W.A. (2004) Endosomal and lysosomal perturbations caused by siRNA-mediated *s*ilencing of Vps34 PI 3'-*k*inase expression in glioblastoma cells. Michigan Microscopy and Microanalysis Society Fall Meeting, Michigan State University, Lansing, MI

Conclusions

The work completed during the past year provides important new insights into the basic mechanisms whereby two key proteins, Beclin and hVps34, function in autophagy and late endosomal protein trafficking. Whereas Vps34 plays a dual role in both autophagy and endosomal protein trafficking, our findings support the hypothesis that Beclin functions selectively to engage the hVps34 PI 3-kinase in the autophagic pathway. An alternative role for Beclin as an essential chaperone or adapter for hVps34 in normal vesicular trafficking has been ruled out by our work. These findings are important because they shed new light on the molecular mechanism whereby Beclin may function as a tumor suppressor. Several lines of evidence support the idea that Beclin is a key component required for the accumulation of autophagosomes in Type II non-apoptotic cell death [10-12]. The latter type of cell death appears to be particularly important for the demise of estrogen receptor positive breast cancer cells treated with tamoxifen or similar compounds [8]. Therefore, the basic investigations into the details of how Beclin regulates autophagosome biogenesis may lay the groundwork for eventual manipulations of Beclin-responsive pathways to enhance the response of breast tumor cells to anti-estrogens. The next step in this line of research will be to isolate the remaining unidentified components in the Beclin-Vps34 complex, so that we can better understand how Beclin may control the targeting or activation of Vps34 when cells are confronted with drugs or environmental conditions that trigger autophagy. These studies will be greatly facilitated by the work completed during the first year of this project which led to the development of a stable ZR-75 breast cancer cell line that lacks Beclin, and a stable MCF7 breast cancer line that over-expresses a FLAG-tagged version of Beclin that can be isolated together with its partners using immuno-affinity techniques.

Reference List

1. S. Volinia et al., *EMBO J.* 14, 3339-3348 (1995).
2. P. E. Row, B. J. Reaves, J. Domin, J. P. Luzio, H. W. Davidson, *Biochem J.* 353, 655-661 (2001).
3. U. Siddhanta, J. McIlroy, A. Shah, Y. Zhang, J. M. Backer, *J.Cell Biol.* 143, 1647-1659 (1998).
4. C. E. Futter, L. M. Collinson, J. M. Backer, C. R. Hopkins, *J.Cell Biol.* 155, 1251-1264 (2001).
5. W. A. Jr. Dunn, *Trends Cell Biol.* 4, 139-143 (1994).
6. D. J. Klionsky and S. D. Emr, *Science* 290, 1717-1721 (2000).
7. Z. Zakeri, W. Bursch, M. Tenniswood, R. A. Lockshin, *Cell Death Differentiat.* 2, 87-96 (1995).
8. W. Bursch et al., *Carcinogenesis* 17, 1595-1607 (1996).
9. B. Levine and D. J. Klionsky, *Dev.Cell* 6, 463-477 (2004).
10. X. H. Liang et al., *Nature* 402, 672-676 (1999).
11. L. Yu et al., *Science* (2004).
12. S. Shimizu et al., *Nat.Cell Biol.* 6, 1221-1228 (2004).

APPENDICES

1) Copy of manuscript submitted to *J. Cell Sci.* (currently in revision)

TITLE: Functional specificity of the mammalian beclin-vps34 pi 3-kinase complex in macroautophagy *versus* endocytosis and lysosomal enzyme sorting

AUTHORS: Xuehuo Zeng, Jean H. Overmeyer and William A. Maltese

2) Copy of manuscript submitted to *Exp. Cell Res.* (currently in revision)

TITLE: Specific function of mammalian Vps34 phosphatidylinositol 3-kinase in late *versus* early endosomes revealed by siRNA-mediated gene silencing.

AUTHORS: Erin E. Johnson, Jean H. Overmeyer, William T. Gunning and William A. Maltese

APPENDIX 1

Functional Specificity of the Mammalian Beclin-Vps34 PI 3-Kinase Complex in Macroautophagy *versus* Endocytosis and Lysosomal Enzyme Sorting

Xuehuo Zeng, Jean H. Overmeyer and William A. Maltese*

Department of Biochemistry and Cancer Biology, Medical University of Ohio, Toledo, OH 43614, USA

* Author for correspondence: (e-mail: wmaltese@mco.edu)

Running title: Functional Specificity of Beclin 1

Key words: Beclin, autophagy, Vps34, phosphatidylinositol-3-kinase, cell death, endocytosis, glioblastoma

Summary

Beclin 1 was originally identified as a novel Bcl-2 interacting protein, but co-immunoprecipitation studies suggest that the major physiological partner for Beclin 1 is the mammalian class-III phosphatidylinositol 3-kinase (PI 3-kinase), mVps34. Beclin 1 has been proposed to function as a tumor suppressor by promoting cellular macroautophagy, a process that is known to depend on mVps34. However, an alternative role for Beclin 1 in modulating normal mVps34-dependent protein trafficking pathways involved in receptor downregulation and lysosomal enzyme sorting has not been ruled out. This possibility was examined in U251 glioblastoma cells where endogenous Beclin 1 was co-immunoprecipitated with mVps34, but not Bcl-2. Suppression of Beclin 1 expression by siRNA-mediated gene silencing blunted the autophagic response of the cells to nutrient deprivation or C2-ceramide. However, other PI 3-kinase dependent trafficking pathways, such as the post-endocytic sorting of the EGF receptor or the proteolytic processing of procathepsin D *en route* from the *trans*-Golgi network to lysosomes, were not affected. Consistent with these findings, depletion of Beclin 1 did not reduce endocytic internalization of a fluid phase marker (HRP) or cause swelling of late endosomal compartments typically seen in cells where the function of mVps34 is impaired. These findings rule out a role for Beclin 1 as an essential chaperone or adapter for mVps34 in normal vesicular trafficking, and they support the hypothesis that Beclin 1 functions as a tumor suppressor by facilitating the engagement of mVps34 in the autophagic pathway.

Introduction

Animal cells utilize macroautophagy as a mechanism for turnover of long-lived proteins, and as a survival strategy under conditions of amino acid deprivation (Dunn, 1994;Klionsky and Emr, 2000). Autophagic vacuoles (autophagosomes) are initially formed from membranes of the endoplasmic reticulum (ER) that surround a region of cytoplasm (Dunn, 1990a;Dunn, 1990b). These structures, bounded by a double membrane, then develop into mature degradative vacuoles (autolysosomes) by progressive fusion with late endosomes and lysosomes (Gordon and Seglen, 1988;Dunn, 1990a;Lawrence and Brown, 1992). Mounting evidence indicates that in addition to promoting short-term survival of nutrient-starved cells, unchecked macroautophagy can also play a pivotal role in type-II programmed cell death, also referred to as autophagic cell death (Lockshin and Zakeri, 2004;Levine and Klionsky, 2004). This type of cell death occurs during embryonic development in connection with tissue remodeling (Zakeri et al., 1995;Melendez et al., 2003). More recently, it has also been described in neurodegenerative diseases (Kegel et al., 2000;Larsen and Sulzer, 2002) and in tumor cells exposed to antineoplastic agents (Bursch et al., 1996;Paglin et al., 2001;Kanzawa et al., 2003;Kanzawa et al., 2004) .

Beclin 1 (hereafter referred to simply as Beclin) is a 60 kDa protein that has been implicated as an important regulator of macroautophagy. It was originally discovered during the course of a yeast two-hybrid screen of a mouse brain cDNA library, using human Bcl-2 as the bait (Liang et al., 1998). The human *beclin* gene has been mapped to a region of chromosome 17q21 that is monoallelically deleted in many breast, ovarian and prostate cancers (Aita et al., 1999). Augmentation of Beclin expression in MCF7 mammary carcinoma cells increases the autophagic response to nutrient deprivation and decreases cell proliferation and tumorgenicity (Liang et al., 1999). Conversely, heterozygous disruption of *beclin* in mice results in an

increased frequency of spontaneous malignancies (Qu et al., 2003). A direct connection between Beclin and autophagic cell death has been demonstrated in two recent studies. In the first, silencing Beclin expression in L929 cells prevented autophagic death triggered by a caspase inhibitor (Yu et al., 2004). In the second, interference with Beclin expression blocked non-apoptotic (autophagic) cell death induced by etoposide treatment of Bax/Bak$^{-/-}$ knockout mouse cells (Shimizu et al., 2004).

Despite the apparent importance of Beclin in the regulation of macroautophagy and non-apoptotic cell death, little is known about the molecular mechanisms that are involved. Studies of the Beclin homolog in *S. cerevisiae* (Vps30/Apg6), indicate that it is part of two distinct protein complexes that contain the PI 3-kinase, Vps34 (Kihara et al., 2001b). One complex functions in post-Golgi sorting of proteases to the vacuole (equivalent to the lysosome), whereas the other complex is essential for macroautophagy and degradation of cytoplasmic proteins under starvation conditions. The importance of Vps34 in protein trafficking is related to the role of its product, phosphatidylinositol 3-phosphate (PI3P), in the membrane recruitment of proteins involved in the vesicle docking and fusion machinery (Wurmser et al., 1999). These proteins typically contain specific PI3P-binding domains termed the FYVE finger (Fruman et al., 1999;Stenmark et al., 2002) or the Phox homology domain (Song et al., 2001;Cheever et al., 2001;Xu et al., 2001;Kanai et al., 2001), and their roles in vesicular transport have been reviewed in recent articles (Simonsen et al., 2001;Deneka and van Der, 2002).

Mammalian cells express a homolog of the yeast Vps34 PI 3-kinase (Volinia et al., 1995) (mVps34). Like the its yeast counterpart, mVps34 appears to be required for the initiation of macroautophagy (Petiot et al., 2000). However, a number of studies have also implicated mVps34 in normal protein trafficking pathways such as the delivery of proteases from the *trans-*

Golgi network (TGN) to the lysosomes (Row et al., 2001), endocytic trafficking and sorting of cell surface receptors (Siddhanta et al., 1998;Tuma et al., 2001;Petiot et al., 2003), and the formation of internal vesicles in multivesicular endosomes (MVE's)(Futter et al., 2001). Since mVps34 can be immunoprecipitated together with Beclin (Kihara et al., 2001a), it is important to consider the possibility that Beclin may influence cell growth and tumorgenicity not only by controlling macroautophagy, but also by functioning as a chaperone or adapter for mVps34 in normal protein trafficking pathways that depend on the production of PI3P. In the present study we addressed this possibility by using siRNA-mediated gene silencing to suppress Beclin expression in U251 glioblastoma cells. The Beclin knockdown (KD) cells exhibited a substantially reduced ability to initiate macroautophagy, but the trafficking of procathepsin D from the TGN to the lysosomes was unaffected. Likewise, near complete suppression of Beclin expression had no effect on cell growth, endocytic uptake of a fluid phase marker, or internalization/degradation of the EGF receptor. These studies provide new insight into the biological significance of the interaction between Beclin and Vps34 PI 3-kinase by showing that it is essential for engagement of Vps34 in the process of macroautophagy, but is dispensable for the normal function of Vps34 in endocytic trafficking or lysosomal enzyme sorting.

Materials and Methods

siRNA-mediated silencing of Beclin

U251 human glioblastoma cells were obtained from the National Cancer Institute Frederick Cancer DCT Tumor Repository (Frederick, MD) and were maintained in Dulbecco's modified Eagle medium (DMEM), supplemented with 10% fetal bovine serum (FBS). The pSUPER.retro.puro vector was obtained from OligoEngine (Seattle, WA). The oligonucleotide sequence used for siRNA interference with Beclin expression corresponded to nucleotides 1201-

1219 (5'-GGCAAGAUUGAAGACACAG-3') downstream of the transcription start site of *beclin* (GeneBank accession number: AF077301), followed by a 9-nucleotide non-complementary spacer (TATCTTGAC) and the reverse complement of the initial 19-nucleotide sequence. A control vector was constructed with a similar insert where the 19-nucleotide sequence had no homology to any known human gene sequence. Retrovirus was produced in 293 GPG packaging cells (Ory et al., 1996) maintained in DMEM + 10% heat-inactivated FBS with 1 μg/ml puromycin, 300 μg/ml G418, and 2 μg/ml doxycycline. For transfection, the 293 GPG cells were seeded at $1.2x10^7$ cells/dish on 100 mm dishes in DMEM containing 10% heat inactivated FBS. Twenty-four hours later 293GPG cells were transfected with the pSuper.retro.puro constructs using Lipofectamine-Plus reagent (Invitrogen, Carlsbad, CA). Forty-eight and seventy-two hours after transfection, the virus-enriched medium was collected and passed through a 0.22 μm filter. Infections of the U251 cells were performed on two sequential days in the presence of 4.0 μg/ml hexadimethrine bromide (Sigma, St. Louis, MO). Twenty four hours after the second infection the cells were trypsinized and re-plated in selection medium containing 1 μg/ml puromycin. After a selection period of 6 days, the surviving cells were pooled and used for studies described in the following sections.

Immunoprecipitation of endogenous Beclin protein complexes

U251 cells were grown to 80% confluence in 100 mm dishes in DMEM with 10% FBS. The cells were washed three times with Hanks balanced salt solution (HBSS), scraped from the dish and homogenized in IP buffer: 50 mM Tris-HCl, pH 7.4, 150 mM NaCl, 1 mM EDTA, 1% Triton X-100, and protease inhibitors. The lysate was centrifuged at 10,000 x g for 15 min at 4 °C and the supernatant solution was incubated with goat polyclonal IgG against Beclin (2 h at 4

°C), followed by 1 h incubation with protein A sepharose beads. The beads were washed three times with IP buffer, twice with phosphate-buffered saline (PBS), and then the immune complexes were eluted from the beads and subjected to SDS-PAGE and immunoblot analysis as described previously (Wilson et al., 1996). Primary antibodies used for immunoblot analysis included mouse monoclonal against Beclin (BD Biosciences, San Diego, CA), rabbit polyclonal against mVps34 (Zymed Laboratories, South San Francisco, CA), mouse monoclonal against Bcl-2, and rabbit polyclonal against Bcl-X_L (Santa Cruz Biotechnology, Santa Cruz, CA).

Subcellular fractionation

Cells were trypsinized, washed in HBSS, suspended in hypotonic buffer (10 mM HEPES, pH 7.5, 1.5 mM $MgCl_2$, 10 mM KCl, 1 mM dithiothreitol and protease inhibitors), and allowed to swell for 10 min. Cells were disrupted with 20 strokes of a Teflon homogenizer and sucrose was added to a final concentration of 0.25 M. The cell lysate was then centrifuged at 100,000 × g for 1 h at 4°C, resulting in soluble (S100) and particulate (P100) fractions.

Immunofluorescence microscopy

Organelle morphology was assessed in control and Beclin KD cells grown on laminin-coated glass coverslips for 24 h. For detection of EEA1, cells were fixed with 3% paraformaldehyde and permeabilized with 0.05% saponin in PBS. For LAMP1 or GM130, cells were fixed with ice-cold methanol for 10 min. All cells were blocked with 10% goat serum in PBS for 30 min and the following monoclonal antibodies were applied for 1 hr in PBS with 10% goat serum: anti-LAMP1 (University of Iowa Developmental Studies Hybridoma Bank, Iowa City, IA), anti-GM130 and anti-EEA1 (BD Biosciences, San Diego, CA). Cells were then washed three times with 10% goat serum in PBS and incubated for 1 hr with Alexa Fluor-568 goat anti-mouse IgG

(Molecular Probes, Eugene, OR). Photomicrographs were taken with a Nikon Eclipse 800 fluorescence microscope equipped with a digital camera. Images were acquired and processed using ImagePro software (Media Cybernetics, Silver Spring, MD).

Induction of autophagy

Macroautophagy was induced by nutrient starvation or exposure to C2-ceramide (N-Acetyl D-erythro-sphingosine; Calbiochem, La Jolla, CA). For starvation, cells were washed with HBSS three times and then incubated in HBSS for 4 h. For C2-ceramide treatment, cells were incubated with 10 μM or 20 μM C2-ceramide in DMEM+0.1% FBS for 24h. Ceramide was dissolved in dimethlysulfoxide (DMSO), and control cultures contained equal amounts of vehicle. The ratio of endogenous LC3 in the unmodified form (LC3-I) and the phosphatidylethanolamine-conjugated form (LC3-II) was determined by immunoblot analysis of whole-cell lysate, using a rabbit polyclonal antibody against LC3 (Kabeya et al., 2000) kindly provided by Dr. Tamotsu Yoshimori.

Detection and quantification of acidic vesicular organelles with acridine orange (AO)

Vital staining of cells with acridine orange (Molecular Probes, Eugene, OR) was performed essentially as described (Paglin *et al.*, 2001). Cells were grown on laminin-coated coverslips (for fluorescence microscopy) or in 96-well plates (for quantification of red fluorescence) and treated with C2-ceramide or vehicle (DMSO) for the indicated time. AO was added for 15 min at a final concentration of 1 μg/ml, and the cells were then washed three times with PBS. Unfixed cells were examined immediately by fluorescence microscopy using a Nikon Eclipse 800 microscope with the red filter set (G-2E/C; excitation 528-553, emission 600-660). Red fluorescence was quantified with a microplate fluorimeter (Molecular Devices, Gemini EM) with excitation and

emission wavelengths set at 488 nm and 655 nm, respectively. To normalize the measurements to the number of cells present in each well, a solution of ethidium bromide was added to a final concentration of 0.2 μM and the fluorescence emitted from the DNA complexes was measured at 530 nm (excitation), 590 nm (emission). The AO red fluorescence was expressed as a ratio to the ethidium bromide (EB) fluorescence.

Cathepsin D processing

Steady-state levels of intracellular cathepsin D were measured in whole-cell lysates by SDS-PAGE and immunoblot analysis, using goat anti-cathepsin D from Santa Cruz Biotechnology (Santa Cruz, CA). To measure the kinetics of cathepsin D processing, U251 cells were pulse-labeled for 30 min in methionine-free DMEM containing 10% FBS and 100 □Ci/ml [^{35}S]methionine (Easy Tag express labeling mix; 1175 Ci/mmol, Perkin Elmer, Boston, MA), then chased for 4 h in DMEM containing 10% FBS, 200 μM methionine and 200 μM cysteine. Cells were washed three times with PBS three times, harvested using a cell scraper, homogenized and solublized in 50 mM Tris-HCl, pH 7.4, 150 mM NaCl, 1% Nonidet P40, 0.5% sodium deoxycholate, 0.1% SDS, 5 mM EDTA. Insoluble material was removed by centrifugation at 100,000 x g for 45 min at 4 °C and the lysates were precleared with protein A Sepharose. Samples were then incubated for 2 h with a polyclonal antibody against cathepsin D (Biodesign International, Saco, Maine). Immune complexes were then collected on protein A sepharose and subjected to SDS-PAGE and fluorography as described previously (Wilson *et al.*, 1996).

Endocytosis of horseradish peroxidase (HRP)

Cells grown to approximately 80% confluence were washed with DMEM and then incubated at 37°C with HRP in (2 mg/ml) in DMEM containing 1% BSA (bovine serum albumin) for the time

periods indicated in the figure. Cells were placed on ice, washed three times with ice-cold PBS containing 1% BSA and one time with PBS. Cells were then scraped into PBS and collected by centrifugation at 390 ×g for 4 min at 4°C. Cell pellets were washed once with PBS and lysed in PBS containing 0.5% Triton X-100. Lysates were cleared by centrifugation for at 10,000 × g for 10 min at 4°C, and equal aliquots were removed for peroxidase assay, using the One-Step Turbo TMB enzyme-linked immunosorbent assay kit (Pierce Chemical, Rockford, IL). After addition of sulfuric acid stop solution, absorbance at 450 nm was measured and the enzyme activity was normalized to total protein, determined using a colorimetric assay (Bio-Rad, Hercules, CA).

Measurement of EGF receptor degradation

Parallel cultures of control or Beclin KD cells were seeded at 200,000 cells/dish on laminin-coated cover slips in 60 mm dishes and grown for 48 h. The cells were then washed with PBS and maintained in serum-free DMEM overnight to allow the epidermal growth factor receptor (EGFR) to accumulate on the cell surface. EGFR internalization was stimulated by incubating the cells 200 ng/ml EGF (Upstate Biotechnology, Charlottesville, VA) in HBSS containing 20 mM HEPES and 0.2% BSA for 30 min or 60 min at room temperature. Immunofluorescence localization of the EGFR was performed using anti-EGFR monoclonal antibody (Upstate Biotechnology), as described earlier for other organelle markers. In a separate study the cells were harvested in SDS sample buffer at 30 min or 70 min after stimulation with EGF, and aliquots containing equal amounts of total cell protein were subjected to SDS-PAGE and immunoblot analysis for EGFR.

Results

Generation of stable Beclin knockdown cell lines

To obtain a cell population in which expression of Beclin was specifically suppressed, cells were infected with a replication-deficient retroviral vector that drives the expression of RNAi sequences and confers puromycin resistance on infected cells (Brummelkamp et al., 2002). Vectors were engineered to contain either an inverted repeat stem-loop sequence matching a unique region of the human *beclin* mRNA, or a "control" sequence that did not match any known GenBank entry. The newly synthesized hairpin RNA is processed into siRNA, triggering the cellular Dicer-mediated degradation of the target *beclin* RNA (Sui et al., 2002). In preliminary tests with several cell lines infected with a GFP reporter construct, the human U251 glioblastoma line showed high initial infection efficiency. Therefore, we chose to use this cell line for studies of Beclin. As shown by the immunoblots in Fig. 1, expression of Beclin was almost undetectable in puromycin-resistant cells that received the Beclin "knockdown" vector (KD), compared with cells that were infected with the control vector. Expression of unrelated proteins (*e.g.*, lactate dehydrogenase, lamin B) was not reduced, indicating that the loss of Beclin expression was not due to a general effect of the siRNA on protein synthesis in the KD cells. In all of the experiments described in this paper, similar immunoblot results were obtained, verifying that expression of Beclin was decreased by 90-95% relative to the parallel control cultures.

Endogenous Beclin forms a complex with mVps34 in U251 glioblastoma cells

Previous studies have indicated that Beclin can be co-immunoprecipitated with mVps34 in HeLa cells (Kihara *et al.*, 2001a). However, Beclin has also been described as a Bcl-2 and Bcl-X_L interacting protein, based on yeast two-hybrid assays and fluorescence resonance energy transfer

analysis of co-expressed proteins (Liang *et al.*, 1998). To determine if these proteins are normal endogenous binding partners for Beclin in U251 glioblastoma cells, Beclin was immunoprecipitated from whole-cell lysate and the associated proteins were probed by immunoblot analysis with antibodies against mVps34, Bcl-2, or Bcl-X_L. Although mVps34, Bcl-2 and Bcl-X_L were all readily detected in the cell lysates, only mVps34 was co-precipitated with Beclin (Fig. 2).

Suppression of Beclin expression interferes with macroautophagy

To assess the consequences of Beclin knockdown for the induction and progression of macroautophagy in U251 cells, we subjected the cells to two established pro-autophagic stimuli; treatment with C_2-ceramide (Scarlatti et al., 2004) and nutrient deprivation (Klionsky *et al.*, 2000;Levine *et al.*, 2004). Microtubule associated protein light-chain 3 (LC3) was used as a molecular marker to monitor autophagosome biogenesis. LC3 is the mammalian homolog of the yeast autophagy protein, Atg8. Like Atg8, LC3 exists in a cytosolic form (LC3-I) and a form that is conjugated to phosphatidylethanolamine (PE) on autophagosome membranes (LC3-II) (Kabeya *et al.*, 2000;Tanida et al., 2002). Initially we attempted to compare autophagosome biogenesis in control *versus* Beclin KD cells by determining the subcellular localization of ectopically expressed GFP-LC3 by fluorescence microscopy of transiently transfected cells. However, the results of this assay were difficult to interpret, due to the low transfection efficiency of U251 cells and the tendency of the overexpressed LC3 to form punctate structures even under normal culture conditions. An alternative approach that avoids overexpression of LC3, entails measuring the ratio of endogenous LC3-II to LC3-I by immunoblot analysis. It is well established that the conversion of LC3-I to LC3-II is closely correlated with the formation of autophagosomes (Kabeya *et al.*, 2000;Tanida et al., 2004). Because LC3-II associates

specifically with the nascent autophagosome isolation membrane and remains on the autophagosome until it matures to an autolysosome, determination of the ratio of LC3-II to LC3-I is now viewed as a definitive marker for activation of the autophagic pathway (Mizushima, 2004;Kirkegaard et al., 2004). As shown in Fig. 3A, nutrient deprivation caused a 3-fold increase in LC3-II/LC3-I in the control U251 cells, but there was comparatively little change in the LC3 ratio in the Beclin KD cells. Ceramide treatment caused an even greater (7-fold) increase in LC3-II/LC3-I in the control cells, with a markedly attenuated response again seen in the Beclin KD cells (Fig. 3B).

The maturation of autophagosomes to autolysosomes is accompanied by a loss of LC3 and an increase in the acidity of the lumen (Mizushima, 2004). Therefore, to assess the relative number of autolysosomes in control *versus* Beclin KD cells, we used an assay that measures supravital staining of acidic compartments with the lysosomotropic agent, acridine orange (AO). When the dye enters an acidic compartment, the protonated form becomes trapped in aggregates that fluoresce bright red or orange (Traganos and Darzynkiewicz, 1994;Paglin *et al.*, 2001;Kanzawa *et al.*, 2003). Previous studies have established that a substantial increase in AO-positive acidic vesicular organelles (AVO's) occurs in conjunction with the induction of macroautophagy in glioblastoma cells (Kanzawa *et al.*, 2003;Kanzawa *et al.*, 2004). As shown in Fig. 4A, a general increase in the intensity of AO-positive structures could be detected in ceramide-treated control cells, but not in the parallel ceramide-treated Beclin KD cells. To obtain a more accurate evaluation of the amount of AO sequestered in acidic compartments, the cells were lysed and the red fluorescence emanating from AO was quantified and normalized to DNA (ethidium bromide fluorescence) (Fig. 4B). The results confirmed that ceramide treatment

stimulated a large increase in the amount of AO sequestered into AVO's in control cells, and that the response to ceramide was greatly reduced in the Beclin KD cells.

Protein trafficking from the TGN to the lysosomes in the Beclin KD cells

Previous studies have indicated that treatment of cells with the PI 3-kinase inhibitor, wortmannin, causes a block in trafficking of procathepsin D from the TGN to the late endosomes and lysosomes (Davidson, 1995;Brown et al., 1995). Similar effects have been reported in cells expressing a kinase-deficient form of mVps34 (Row *et al.*, 2001). In light of the association between Beclin and mVps34, we wished to determine if cells lacking normal amounts of Beclin would exhibit any defects in this PI 3-kinase-dependent trafficking pathway. Newly synthesized procathepsin D (51-53 kDa) associates with the cation-independent mannose 6-phosphate receptor (M6PR) in the TGN and is delivered to the endosomal compartment, where it is activated by removal of the pro-peptide to generate an intermediate form that migrates at 47-48 kD on SDS gels. The final step in cathepsin D processing is completed in the lysosomes, where the intermediate is cleaved to the mature form, which contains two non-covalently linked chains of 31 kDa and 14 kDa (Rijnboutt et al., 1992;Delbruck et al., 1994). As shown by the immunoblots in Fig. 5A, the steady-state levels of the 53 kDa procathepsin D, the 47 kDa intermediate and the 31 kDa mature cathepsin D were similar in the control and Beclin KD cells. This method can readily detect perturbations in procathepsin D processing, as illustrated in cells treated with ammonium chloride to raise the pH of the endosomal and lysosomal compartments (Fig. 5A).

To obtain a more direct assessment of the processing of newly synthesized procathepsin D, we performed a pulse-chase analysis (Fig. 5B). When ^{35}S-methionine-labled cathepsin D was immunoprecipitated after a 30 min pulse, nearly all of the radiolabeled protein was in the 53 kDa

pro form in both control and KD cells. After a 4-h chase, the mature 31 kDa cathepsin D was the predominant form detected in both control and Beclin KD cells, with no residual 53 kDa procathepsin D and only a small amount of the 47 kDa endosomal intermediate. By comparison, cells treated with ammonium chloride generated no mature cathepsin D during the same time period. Immunoprecipitation of the culture medium, followed by prolonged film exposure, revealed a small amount of secreted procathepsin D, but this did not vary between the control and Beclin KD cells (not shown). These results indicate that Beclin association with mVps34 is not required for normal PI 3-kinase dependent trafficking of procathepsin D from the TGN to the endosomal and lysosomal compartments in U251 cells.

Endocytic trafficking in the Beclin KD cells

In addition to disrupting trafficking between the TGN and lysosome, wortmannin causes marked swelling of late endosome compartments (Reaves et al., 1996;Fernandez-Borja et al., 1999). This appears to be due to failure of inward vesiculation of multivesicular endosomes, without a compensatory decrease in endocytic membrane influx (Futter *et al.*, 2001). We have recently observed a similar enlargement of vesicular compartments containing the late endosome/lysosome membrane marker, LAMP1, when mVps34 expression was silenced in U251cells (unpublished). In contrast to these findings, immunofluorescence microscopy of the Beclin KD cells revealed no detectable changes in the morphology or distribution of molecular markers for early endosomes (EEA1), late endosomes/lysosomes (LAMP1) or Golgi membranes (GM130) (Fig. 6). To directly assess the endocytic transport pathway, we measured the cellular uptake of the fluid marker, HRP (Fig. 7). The results did not reveal any consistent perturbation of HRP endocytosis in cells lacking Beclin.

To further explore the endocytic pathway, we followed the fate of activated EGFR. In serum-deprived cells grown in the absence of EGF, degradation of EGFR is minimal and receptors accumulate on the cell surface. However, upon addition of EGF, the receptors are rapidly activated by tyrosine phosphorylation in the C-terminal cytoplasmic domain and the EGF-EGFR complexes are internalized into clathrin-coated early endosomes. Down-regulation of activated receptors depends on their delivery to multivesicular endosomes (MVE's), where receptor complexes are sorted into internal vesicles that are ultimately degraded when the late endosomes fuse with lysosomes (Katzmann et al., 2002). Localization of EGFR by immunofluorescence in serum-starved control and Beclin KD cells showed that most of the receptors were indeed present in the peripheral cell membrane (Fig. 8A). Within 30 min after addition of EGF, most of the receptors were found in small internal vesicles diffusely arrayed throughout the cytoplasm, typical of early endosomes and MVE's (Fig. 8A). By 70 min, most of the EGFR-positive structures were clustered in the juxtanuclear region in a pattern typical of late endosomes or lysosomes. At all of these stages we were unable to discern any consistent differences in EGFR localization between the control and Beclin KD cells (Fig. 8A). To examine degradation of the EGFR, immunoblot analysis of total EGFR was performed at intervals after addition of EGF. The results indicate that time course of receptor degradation was nearly identical in the Beclin KD cells compared with the controls (Fig. 8B).

Finally, since disruption of vesicular trafficking would be expected to have consequences for cell proliferation, we compared the rate of cell proliferation for control and Beclin KD cells (Fig. 9). Consistent with the normal morphology (Fig. 6) and endocytic internalization of HRP or EGFR (Figs. 7 & 8), the suppression of Beclin expression had no detectable effect on proliferation of U251 cells (Fig. 9).

Discussion

Beclin is an interacting partner for the mammalian Class-III PI 3-kinase, mVps34. Previous studies have established that mVps34 is required for macroautophagy in nutrient starved cells (Petiot *et al.*, 2000), for normal lysosomal enzyme sorting and protein trafficking in the endocytic pathway (Row *et al.*, 2001;Futter *et al.*, 2001;Petiot *et al.*, 2003), and for cell cycling (Siddhanta *et al.*, 1998). The studies presented in this report are the first to test the hypothesis that Beclin may serve as an essential chaperone or adapter for the function of mVps34 in pathways beyond macroautophagy. The results indicate that Beclin is required specifically for the function of mVps34 in the autophagy pathway, but not for the normal functions of this PI 3-kinase in TGN → lysosome trafficking, endocytosis or cell proliferation. These findings contrast with previous studies of the Beclin homolog, Vps30 (Atg6), in *S. cerevisiae.* In those studies Vps30 interaction with Vps34 was found to be required for *both* starvation-induced autophagy (Seaman et al., 1997;Kametaka et al., 1998) and vesicular transport of carboxypeptidase Y (CPY) from the Golgi compartment to the vacuole (Klionsky et al., 1990). The dual role of Vps30 in yeast can be attributed to its assembly into two distinct protein complexes (Kihara *et al.*, 2001b). In the autophagy pathway, Vps30 is linked to Vps34 through an interaction with a novel bridging protein, Atg14, whereas in the Golgi→ vacuole pathway a different linker protein, Vps38, mediates this interaction. Several lines of evidence suggest that the mammalian Beclin-Vps34 complex may be fundamentally different from these yeast Vps30-Vps34 complexes. First, in *vps30*-defective yeast, Beclin can complement Vps30 in the autophagy pathway, but not in the vacuolar protein-sorting pathway (Liang *et al.*, 1999). This would be consistent with our finding that Beclin does not function in post-Golgi sorting of

cathepsin D. Second, homologs of the bridging proteins, Atg14 and Vps38, have not yet been identified in mammalian cells. Finally, Vps30 is significantly larger (557 aa) than human Beclin (450 aa), owing mainly to sequence variations in the N-terminal and C-terminal regions outside the central coiled-coil and myosin-like domains. Taken together, these observations suggest that structural features that promote interaction of the yeast Vps30-Vps34 complex with vesicular sorting pathways have been lost in Beclin, while those that promote interaction with the autophagy pathway are conserved.

PI3P is distributed throughout cellular endomembranes, where it serves to recruit a variety of proteins implicated in the regulation of vesicular transport and intracellular protein sorting (Simonsen *et al.*, 2001;Corvera, 2001). Some of these proteins contain a Phox homology phosphoinositide-binding domain (Song *et al.*, 2001;Cheever *et al.*, 2001;Xu *et al.*, 2001;Kanai *et al.*, 2001), while others contain a structural motif termed the FYVE finger, which binds to PI3P with high affinity (Wurmser *et al.*, 1999;Fruman *et al.*, 1999;Corvera et al., 1999). Little is known about the molecular events that direct the targeting of the mVps34 PI-3-kinase to specific subcellular compartments. Like its yeast counterpart, mVps34 appears to associate with intracellular membranes through interaction with a myristylated adapter, p150 (mVps15) (Volinia *et al.*, 1995;Panaretou et al., 1997). There is some evidence that recruitment of mVps34 to endosomal membranes is facilitated by specific Rab GTPases (*e.g.*, Rab5, Rab7) that can bind to p150 (mVps15) (Murray et al., 2002;Stein et al., 2003). Once it is associated with the membrane, mVps34 presumably generates the PI3P required for membrane association of FYVE-domain proteins such as the Rab effectors, EEA1 and Rabenosyn-5 (Simonsen et al., 1998;De Renzis et al., 2002), and the PI3P 5-kinase, PIKfyve (Ikonomov et al., 2003). Our finding that Beclin can be substantially depleted from mammalian cells without any detectable

consequences for endosome morphology, EEA1 distribution, or endocytic trafficking leads us to conclude that Beclin is not required for the targeting or recruitment of mVps34 to endosomal membranes. On the other hand, our studies clearly implicate Beclin in one or more key steps required for generating a central component of the pre-autophagosome protein complex, LC-II.

Several reviews have summarized the recent advances in understanding the pre-autophagosomal protein assemblies involved in initiating the formation of the isolation membrane (Wang and Klionsky, 2003;Kirkegaard *et al.*, 2004;Marino and Lopez-Otin, 2004). The conjugation of LC3 (Atg8) to PE, generating LC3-II, occupies a central position in this scheme. LC3 is first cleaved by a cysteine protease (Atg4/autophagin) to expose a C-terminal glycine. The protein is then conjugated sequentially, first to Atg7, then to Atg3, before the final conjugation to PE on the pre-autophagosome membrane. The lipidated form of LC3 appears to play a key role in recruiting at least one other essential oligomeric protein complex (Atg12-Atg5, Atg16) to the pre-autophagosome membrane. Therefore, our observation that Beclin is required for the formation of LC3-II implies that Beclin functions in the earliest steps required for autophagosome biogenesis, rather than in the later maturation events involving fusion with endosomes or lysosomes. Since inhibitors of PI 3-kinase have been reported to cause a reduction in LC3-II production (Aki et al., 2003), we believe that the attenuated production of LC3-II observed in starved or ceramide-treated Beclin KD cells is related to an impaired ability of mVps34 to function in the autophagy pathway without Beclin. The molecular basis for the apparent requirement for PI3P in the autophagic process in mammalian cells remains to be determined. However, recent studies have described an autophagy-linked FYVE-domain protein, Alfy (Simonsen et al., 2004), and a Rab GTPase, Rab24, (Munafo and Colombo, 2002) associated with autophagosomes. These findings raise the intriguing possibility that PI3P-

dependent molecular assemblies not unlike those described on early endosomes (De Renzis *et al.*, 2002) may also play a role in the formation and/or maturation of autophagosomes.

The present results have particular relevance for understanding the mechanism whereby Beclin may function as a tumor suppressor (Liang *et al.*, 1999;Qu *et al.*, 2003). As mentioned in the introduction, several lines of evidence support the idea that the Beclin is a key component required for the accumulation of autophagosomes in type II non-apoptotic cell death (Scarlatti *et al.*, 2004;Yu *et al.*, 2004;Shimizu *et al.*, 2004). Nevertheless, without knowing if Beclin interaction with mVps34 is also required for the function of this PI 3-kinase in normal vesicular trafficking pathways, some question has remained as to whether or not the apparent tumor suppressing activity of Beclin is directly related to its role in autophagy. For example, it is possible to envision an alternative model wherein loss of Beclin might potentiate growth factor signaling pathways by disrupting mVps34-dependent steps required for post-endocytic sorting and lysosomal degradation of activated receptors (Futter et al., 1996;Futter *et al.*, 2001). The results of the present studies argue against this possibility by showing that Beclin is not required for the normal function of mVps34 in endocytosis, EGFR degradation, post-Golgi sorting of lysosomal proteins, or cell proliferation. We therefore propose that a primary function of Beclin is to facilitate the interaction of mVps34 PI 3-kinase with specific effectors on the pre-autophagosomal isolation membrane in response to pro-autophagic conditions or death signals.

A major unsolved puzzle regarding Beclin is the biological significance of its reported interaction with the anti-apoptotic proteins Bcl-2 and Bcl-X_L, which have no known connection to mVps34-mediated protein trafficking or the pre-autophagosomal Atg protein complexes. Interest in this question has intensified with the recent observation that etoposide treatment induces autophagic cell death instead of apoptosis in wild-type or Bax/Bak $^{-/-}$ mouse embryonic

fibroblasts overexpressing Bcl-2 or Bcl-X_L (Shimizu *et al.*, 2004). The interaction between Beclin and Bcl-2 first observed in yeast two-hybrid assays was confirmed by FRET analysis of the two proteins overexpressed in COS cells (Aita *et al.*, 1999). Similarly, we have found it easy to observe an interaction between these proteins in pull-down assays using transfected 293 cells overexpressing both FLAG-Beclin and Bcl-2 (unpublished). However, as shown in this study, we have been unable to detect an interaction between endogenous Beclin and Bcl-2 or Bcl-X_L under conditions that allow co-immunoprecipitation of Beclin with mVps34. Our findings are consistent with those of Kihara *et al.* (Kihara *et al.*, 2001a), who demonstrated that all of the endogenous Beclin in Hela cells could be co-immunoprecipitated with an antibody against mVps34. Nevertheless, these studies do not completely rule out the possibility that low-affinity interactions may occur between membrane- bound Bcl-2 or Bcl-X_L and the Beclin-mVps34 complex. Such interactions might be lost in the detergent-containing buffers typically used for immunoprecipitation. Alternatively, the interactions between Beclin and Bcl-2 might be more prominent in specific cell types or under certain metabolic conditions. This will be an important topic for future study.

Acknowledgements: We thank Jane Ding for technical assistance and Dr. Tamotsu Yoshimori for providing the antibody against LC3. This work was supported by a U.S. Department of Defense Breast Cancer Research Program Grant, BC031231, to W.A.M.

References

Aita,V.M., Liang,X.H., Murty,V.V., Pincus,D.L., Yu,W., Cayanis,E., Kalachikov,S., Gilliam,T.C., and Levine,B. (1999) Cloning and genomic organization of beclin 1, a candidate tumor suppressor gene on chromosome 17q21. *Genomics* **59**, 59-65.

Aki,T., Yamaguchi,K., Fujimiya,T., and Mizukami,Y. (2003) Phosphoinositide 3-kinase accelerates autophagic cell death during glucose deprivation in the rat cardiomyocyte-derived cell line H9c2. *Oncogene* **22**, 8529-8535.

Brown,W.J., DeWald,D.B., Emr,S.D., Plutner,H., and Balch,W.E. (1995) Role for phosphatidylinositol 3-kinase in the sorting and transport of newly synthesized lysosomal enzymes in mammalian cells. *J. Cell Biol.* **130**, 781-796.

Brummelkamp,T.R., Bernards,R., and Agami,R. (2002) A system for stable expression of short interfering RNAs in mammalian cells. *Science* **296**, 550-553.

Bursch,W., Ellinger,E., Kienzl,H., Torok,L., Pandey,S., Sikorska,M., Walker,R., and Hermann,R.S. (1996) Active cell death induced by the anti-estrogens tamoxifin and ICI 164 384 in human mammary carcioma cells (MCF-7) in culture: the role of autophagy. *Carcinogenesis* **17**, 1595-1607.

Cheever,M.L., Sato,T.K., de Beer,T., Kutateladze,T.G., Emr,S.D., and Overduin,M. (2001) Phox domain interaction with PtdIns(3)P targets the Vam7 t-SNARE to vacuole membranes. *Nat. Cell Biol.* **3**, 613-618.

Corvera,S., D'Arrigo,A., and Stenmark,H. (1999) Phosphoinositides in membrane traffic. *Curr. Opin. Cell Biol.* **11**, 460-465.

Corvera,S. (2001) Phosphatidylinositol 3-kinase and the control of endosome dynamics: New players defined by structural motifs. *Traffic* **2**, 859-866.

Davidson,H.W. (1995) Wortmannin causes mistargeting of procathepsin D. Evidence for the involvement of a phosphatidylinositol 3-kinase in vesicular transport to lysosomes. *J. Cell Biol.* **130**, 797-805.

De Renzis,S., Sonnichsen,B., and Zerial,M. (2002) Divalent Rab effectors regulate the sub-compartmental organization and sorting of early endosomes. *Nat. Cell Biol.* **4**, 124-133.

Delbruck,R., Desel,C., von Figura,K., and Hille-Rehfeld,A. (1994) Proteolytic processing of cathepsin D in prelysosomal organelles. *Eur. J. Cell Biol.* **64**, 7-14.

Deneka,M. and van Der,S.P. (2002) 'Rab'ing up endosomal membrane transport. *Nat. Cell Biol.* **4**, E33-E35.

Dunn,W.A.Jr. (1990a) Studies on the mechanisms of autophagy: Formation of the autophagic vacuole. *J. Cell Biol.* **110**, 1923-1933.

Dunn,W.A.Jr. (1990b) Studies on the mechanisms of autophagy: Maturation of the autophagic vacuole. *J. Biol. Chem.* **110**, 1935-1945.

Dunn,W.A.Jr. (1994) Autophagy and related mechanisms of lysosome-mediated protein degradation. *Trends Cell Biol.* **4**, 139-143.

Fernandez-Borja,M., Wubbolts,R., Calafat,J., Janssen,H., Divecha,N., Dusseljee,S., and Neefjes,J. (1999) Multivesicular body morphogenesis requires phosphatidylinositol 3-kinase activity. *Curr. Biol.* **9**, 55-58.

Fruman,D.A., Rameh,L.E., and Cantley,L.C. (1999) Phosphoinositide binding domains: embracing 3-phosphate. *Cell*, **97**, 817-820.

Futter,C.E., Collinson,L.M., Backer,J.M., and Hopkins,C.R. (2001) Human VPS34 is required for internal vesicle formation within multivesicular endosomes. *J. Cell Biol.* **155**, 1251-1264.

Futter,C.E., Pearse,A., Hewlett,L.J., and Hopkins,C.R. (1996) Multivesicular endosomes containing internalized EGF-EGF receptor complexes mature and then fuse directly with lysosomes. *J. Cell Biol.* **132**, 1011-1023.

Gordon,P. and Seglen,P.O. (1988) Prelysosomal convergence of autophagic and endocytic pathways. *Biochem Biophy Res Commun.* **151**, 40-47.

Ikonomov,O.C., Sbrissa,D., Foti,M., Carpentier,J.L., and Shisheva,A. (2003) PIKfyve controls fluid phase endocytosis but not recycling/degradation of endocytosed receptors or

sorting of procathepsin D by regulating multivesicular body morphogenesis. *Mol. Biol. Cell* **14**, 4581-4591.

Kabeya,Y., Mizushima,N., Ueno,T., Yamamoto,A., Kirisako,T., Noda,T., Kominami,E., Ohsumi,Y., and Yoshimori,T. (2000) LC3, a mammalian homologue of yeast apg8p, is localized in autophagosome membranes after processing. *EMBO J.* **19**, 5720-5728.

Kametaka,S., Okano,T., Ohsumi,M., and Ohsumi,Y. (1998) Apg14p and Apg6/Vps30p form a protein complex essential for autophagy in the yeast, Saccharomyces cerevisiae. *J. Biol. Chem.* **273**, 22284-22291.

Kanai,F., Liu,H., Field,S.J., Akbary,H., Matsuo,T., Brown,G.E., Cantley,L.C., and Yaffe,M.B. (2001) The PX domains of p47phox and p40phox bind to lipid products of PI(3)K. *Nat. Cell Biol.* **3**, 675-678.

Kanzawa,T., Germano,I.M., Komata,T., Ito,H., Kondo,Y., and Kondo,S. (2004) Role of autophagy in temozolomide-induced cytotoxicity for malignant glioma cells. *Cell Death. Differ.* **11**, 448-457.

Kanzawa,T., Kondo,Y., Ito,H., Kondo,S., and Germano,I. (2003) Induction of autophagic cell death in malignant glioma cells by arsenic trioxide. *Cancer Res.* **63**, 2103-2108.

Katzmann,D.J., Odorizzi,G., and Emr,S.D. (2002) Receptor downregulation and multivesicular-body sorting. *Nat. Rev. Mol. Cell Biol.* **3**, 893-905.

Kegel,K.B., Kim,M., Sapp,E., McIntyre,C., Castano,J.G., Aronin,N., and DiFiglia,M. (2000) Huntingtin expression stimulates endosomal-lysosomal activity, endosome tubulation, and autophagy. *J. Neurosci.* **20**, 7268-7278.

Kihara,A., Kabeya,Y., Ohsumi,Y., and Yoshimori,T. (2001a) Beclin-phosphatidylinositol 3-kinase complex functions at the trans-Golgi network. *EMBO Rep.* **2**, 330-335.

Kihara,A., Noda,T., Ishihara,N., and Ohsumi,Y. (2001b) Two distinct Vps34 phosphatidylinositol 3-kinase complexes function in autophagy and carboxypeptidase Y sorting in Saccharomyces cerevisiae. *J. Cell Biol.* **152**, 519-530.

Kirkegaard,K., Taylor,M.P., and Jackson,W.T. (2004) Cellular autophagy: surrender, avoidance and subversion by microorganisms. *Nat. Rev. Microbiol.* **2**, 301-314.

Klionsky,D.J. and Emr,S.D. (2000) Autophagy as a regulated pathway of cellular degradation. *Science* **290**, 1717-1721.

Klionsky,D.J., Herman,P.K., and Emr,S.D. (1990). The fungal vacuole: composition, function, and biogenesis. *Microbiol. Rev.* **54**, 266-292.

Larsen,K.E. and Sulzer,D. (2002) Autophagy in neurons: a review. *Histol. Histopathol.* **17**, 897-908.

Lawrence,B. and Brown,W. (1992) Autophagic vacuoles rapidly fuse with pre-existing lysosomes in cultured hepatocytes. *J Cell Sci* **102**, 515-526.

Levine,B. and Klionsky,D.J. (2004) Development by self-digestion: molecular mechanisms and biological functions of autophagy. *Dev. Cell* **6**, 463-477.

Liang,X.H., Jackson,S., Seaman,M., Brown,K., Kempkes,B., Hibshoosh,H., and Levine,B. (1999) Induction of autophagy and inhibition of tumorigenesis by beclin 1. *Nature* **402**, 672-676.

Liang,X.H., Kleeman,L.K., Jiang,H.H., Gordon,G., Goldman,J.E., Berry,G., Herman,B., and Levine,B. (1998) Protection against fatal Sindbis virus encephalitis by beclin, a novel Bcl-2-interacting protein. *J. Virol.* **72**, 8586-8596.

Lockshin,R.A. and Zakeri,Z. (2004) Apoptosis, autophagy, and more. *Int. J Biochem. Cell Biol.* **36**, 2405-2419.

Marino,G. and Lopez-Otin,C. (2004) Autophagy: molecular mechanisms, physiological functions and relevance in human pathology. *Cell Mol. Life Sci.* **61**, 1439-1454.

Melendez,A., Talloczy,Z., Seaman,M., Eskelinen,E.L., Hall,D.H., and Levine,B. (2003) Autophagy genes are essential for dauer development and life-span extension in C. elegans. *Science* **301**, 1387-1391.

Mizushima,N. (2004) Methods for monitoring autophagy. *Int. J Biochem. Cell Biol.* **36**, 2491-2502.

Munafo,D.B. and Colombo,M.I. (2002). Induction of autophagy causes dramatic changes in the subcellular distribution of GFP-Rab24. *Traffic* **3**, 472-482.

Murray,J.T., Panaretou,C., Stenmark,H., Miaczynska,M., and Backer,J.M. (2002) Role of Rab5 in the recruitment of hVps34/p150 to the early endosome. *Traffic* **3**, 416-427.

Ory,D.S., Neugeboren,B.A., and Mulligan,R.C. (1996) A stable human-derived packaging cell line for production of high titer retrovirus/vesicular stomatitis virus G pseudotypes. *Proc. Natl. Acad. Sci U. S. A* **93**, 11400-11406.

Paglin,S., Hollister,T., Delohery,T., Hackett,N., McMahill,M., Sphicas,E., Domingo,D., and Yahalom,J. (2001) A novel response of cancer cells to radiation involves autophagy and formation of acidic vesicles. *Cancer Res.* **61**, 439-444.

Panaretou,C., Domin,J., Cockcroft,S., and Waterfield,M.D. (1997) Characterization of p150, an adaptor protein for the human phosphatidylinositol (PtdIns) 3-kinase. Substrate presentation by phosphatidylinositol transfer protein to the p150 Ptdins 3-kinase complex. *J. Biol. Chem.* **272**, 2477-2485.

Petiot,A., Faure,J., Stenmark,H., and Gruenberg,J. (2003) PI3P signaling regulates receptor sorting but not transport in the endosomal pathway. *J. Cell Biol.* **162**, 971-979.

Petiot,A., Ogier-Denis,E., Blommaart,E.F., Meijer,A.J., and Codogno,P. (2000) Distinct classes of phosphatidylinositol 3'-kinases are involved in signaling pathways that control macroautophagy in HT-29 cells. *J. Biol. Chem.* **275**, 992-998.

Qu,X., Yu,J., Bhagat,G., Furuya,N., Hibshoosh,H., Troxel,A., Rosen,J., Eskelinen,E.L., Mizushima,N., Ohsumi,Y., Cattoretti,G., and Levine,B. (2003) Promotion of tumorigenesis by heterozygous disruption of the beclin 1 autophagy gene. *J. Clin. Invest.* **112**, 1809-1820.

Reaves,B.J., Bright,N.A., Mullock,B.M., and Luzio,J.P. (1996) The effect of wortmannin on the localisation of lysosomal type I integral membrane glycoproteins suggests a role for phosphoinositide 3-kinase activity in regulating membrane traffic late in the endocytic pathway. *J. Cell Sci.* **109**, 749-762.

Rijnboutt,S., Stoorvogel,W., Geuze,H.J., and Strous,G.J. (1992) Identification of subcellular compartments involved in biosynthetic processing of cathepsin D. *J. Biol. Chem.* **267**, 15665-15672.

Row,P.E., Reaves,B.J., Domin,J., Luzio,J.P., and Davidson,H.W. (2001) Overexpression of a rat kinase-deficient phosphoinositide 3-kinase, Vps34p, inhibits cathepsin D maturation. *Biochem J.* **353**, 655-661.

Scarlatti,F., Bauvy,C., Ventruti,A., Sala,G., Cluzeaud,F., Vandewalle,A., Ghidoni,R., and Codogno,P. (2004) Ceramide-mediated macroautophagy involves inhibition of protein kinase B and upregulation of Beclin 1. *J. Biol. Chem.*.

Seaman,M.N., Marcusson,E.G., Cereghino,J.L., and Emr,S.D. (1997) Endosome to Golgi retrieval of the vacuolar protein sorting receptor, Vps10p, requires the function of the VPS29, VPS30, and VPS35 gene products. *J. Cell Biol.* **137**, 79-92.

Shimizu,S., Kanaseki,T., Mizushima,N., Mizuta,T., Arakawa-Kobayashi,S., Thompson,C.B., and Tsujimoto,Y. (2004) Role of Bcl-2 family proteins in a non-apoptotic programmed cell death dependent on autophagy genes. *Nat. Cell Biol.* **6**, 1221-1228.

Siddhanta,U., McIlroy,J., Shah,A., Zhang,Y., and Backer,J.M. (1998) Distinct roles for the p110alpha and hVPS34 phosphatidylinositol 3'- kinases in vesicular trafficking, regulation of the actin cytoskeleton, and mitogenesis. *J. Cell Biol.* **143**, 1647-1659.

Simonsen,A., Birkeland,H.C., Gillooly,D.J., Mizushima,N., Kuma,A., Yoshimori,T., Slagsvold,T., Brech,A., and Stenmark,H. (2004) Alfy, a novel FYVE-domain-containing protein associated with protein granules and autophagic membranes. *J Cell Sci.* **117**, 4239-4251.

Simonsen,A., Lippe,R., Christoforidis,S., Gaullier,J.M., Brech,A., Callaghan,J., Toh,B.H., Murphy,C., Zerial,M., and Stenmark,H. (1998) EEA1 links PI(3)K function to Rab5 regulation of endosome fusion. *Nature* **394**, 494-498.

Simonsen,A., Wurmser,A.E., Emr,S.D., and Stenmark,H. (2001) The role of phosphoinositides in membrane transport. *Curr. Opin. Cell Biol.* **13**, 485-492.

Song,X., Xu,W., Zhang,A., Huang,G., Liang,X., Virbasius,J.V., Czech,M.P., and Zhou,G.W. (2001) Phox homology domains specifically bind phosphatidylinositol phosphates. *Biochemistry* **40**, 8940-8944.

Stein,M.P., Feng,Y., Cooper,K.L., Welford,A.M., and Wandinger-Ness,A. (2003) Human VPS34 and p150 are Rab7 interacting partners. *Traffic.* **4**, 754-771.

Stenmark,H., Aasland,R., and Driscoll,P.C. (2002) The phosphatidylinositol 3-phosphate-binding FYVE finger. *FEBS Lett.* **513**, 77-84.

Sui,G., Soohoo,C., Affar,e.B., Gay,F., Shi,Y., Forrester,W.C., and Shi,Y. (2002) A DNA vector-based RNAi technology to suppress gene expression in mammalian cells. *Proc. Natl. Acad. Sci. U. S. A.* **99**, 5515-5520.

Tanida,I., Ueno,T., and Kominami,E. (2004) LC3 conjugation system in mammalian autophagy. *Int. J Biochem. Cell Biol.* **36**, 2503-2518.

Tanida,I., Tanida-Miyake,E., Komatsu,M., Ueno,T., and Kominami,E. (2002) Human Apg3p/Aut1p homologue is an authentic E2 enzyme for multiple substrates, GATE-16, GABARAP, and MAP-LC3, and facilitates the conjugation of hApg12p to hApg5p. *J. Biol. Chem.* **277**, 13739-13744.

Traganos,F. and Darzynkiewicz,Z. (1994). Lysosomal proton pump activity: supravital cell staining with acridine orange differentiates leukocyte subpopulations. *Methods Cell Biol.* **41**, 185-194.

Tuma,P.L., Nyasae,L.K., Backer,J.M., and Hubbard,A.L. (2001) Vps34p differentially regulates endocytosis from the apical and basolateral domains in polarized hepatic cells. *J Cell Biol.* **154**, 1197-1208.

Volinia,S., Dhand,R., Vanhaesebroeck,B., MacDougall,L.K., Stein,R., Zvelebil,M.J., Domin,J., Panaretou,C., and Waterfield,M.D. (1995) A human phosphatidylinositol 3-kinase complex related to the yeast Vps34p-Vps15p protein sorting system. *EMBO J.* **14**, 3339-3348.

Wang,C.W. and Klionsky,D.J. (2003) The molecular mechanism of autophagy. *Mol. Med.* **9**, 65-76.

Wilson,A.L., Erdman,R.A., and Maltese,W.A. (1996). Association of Rab1B with GDP-dissociation inhibitor (GDI) is required for recycling but not initial membrane targeting of the Rab protein. *J. Biol. Chem.* **271**, 10932-10940.

Wurmser,A.E., Gary,J.D., and Emr,S.D. (1999) Phosphoinositide 3-kinases and their FYVE domain-containing effectors as regulators of vacuolar/lysosomal membrane trafficking pathways. *J. Biol. Chem.* **274**, 9129-9132.

Xu,Y., Hortsman,H., Seet,L., Wong,S.H., and Hong,W. (2001) SNX3 regulates endosomal function through its PX-domain-mediated interaction with PtdIns(3)P. *Nat. Cell Biol.* **3**, 658-666.

Yu,L., Alva,A., Su,H., Dutt,P., Freundt,E., Welsh,S., Baehrecke,E.H., and Lenardo,M.J. (2004) Regulation of an ATG7-beclin 1 program of autophagic cell death by caspase-8. *Science* **304**, 1500-1502.

Zakeri,Z., Bursch,W., Tenniswood,M., and Lockshin,R.A. (1995) Cell death:programmed, apoptosis,necrosis or other? *Cell Death Differentiat.* **2**, 87-96.

Figure Legends

Fig. 1. siRNA-mediated suppression of Beclin expression in U251 glioma cells. U251 cells infected with retroviral vectors and surviving after 6 days in medium containing 1 μg/ml puromycin were pooled to generate stable cell lines. Beclin expression in control and Beclin knockdown (KD) cells was detected by immunoblot analysis with a monoclonal anti-Beclin IgG as described in the Methods.

Fig. 2. Immunoprecipitated Beclin complex from U251 cells contains mVps34 but not Bcl-2 or Bcl-X_L. Cells lysates were prepared from parallel cultures as described in the Methods and 10% of each lysate was saved for immunoblot analysis. The remainder of each lysate was immunoprecipitated with either IgG against Beclin or a 'control' IgG against an unrelated protein (SPARC, Santa Cruz Biotechnology). Equal aliquots of the immune complexes eluted from protein A sepharose beads were probed by immunoblot analysis using the antibodies indicated at the left of each panel. The band appearing just below Beclin in the upper panel is a non-specific cross-reacting protein.

Fig. 3. Suppression of Beclin expression impairs the autophagy-associated posttranslational processing of endogenous LC3-I to LC3-II. (A) Cells were incubated in DMEM+ 10% FBS (normal) or HBSS (starved) for 4 h. (B) Cells were treated with vehicle or 10 μM C2-ceramide (+ ceramide) for 24 h. All cells were subjected to SDS-PAGE and immunoblot analysis to detect the endogenous cytosolic LC3-I and the PE-conjugated LC3-II. The ratios of LC3-II to LC3-I represented in the bar graphs were determined from scans of the blots performed with a Kodak 440CF Image Station.

Fig. 4. Accumulation of acidic vesicular organelles (AVO's) induced by ceramide treatment is impaired in Beclin KD cells. (A) Control and Beclin KD cells were maintained for 24 h in medium with or without 10 μM C2-ceramide, as indicated. Cells were then incubated with acridine orange (AO) and examined by fluorescence microscopy, using a filter combination to detect red fluorescence. All digital micrographs were taken at the same exposure setting. The scale bar represents 50 μm. (B) Control and Beclin KD cells were treated with 0, 10 or 20 μM C2-ceramide for 24 h and incubated with AO. The relative amount of AO trapped in vesicular compartments (red fluorescence; excitation at 488 nm, emission at 655nm) was measured and normalized to cellular DNA detected with ethidium bromide (EB). The data represent the mean ± S.E. of three determinations from parallel cultures.

Fig. 5. Suppression of Beclin expression does not impede lysosomal enzyme sorting as measured by cathepsin D processing. (A) Immunoblot analysis was performed on endogenous cathepsin D in whole cell lysates from control and Beclin KD cells. To demonstrate inhibition of cathepsin D processing, a separate control culture was incubated with 10 mM NH_4Cl for 24 h prior to harvest. Equal amounts of protein were loaded in each lane. The part of the blot above the dashed line was exposed 7 times longer than the lower portion, to permit detection of the precursor forms of cathepsin D. (B) Cells were labeled with 100 μCi/ml ^{35}S-methionine, then harvested immediately or chased in medium with unlabeled methionine for 4 h. A separate control culture was incubated with 15 mM NH_4Cl during the 4-h chase. Cathepsin D was immunoprecipitated and subjected to SDS-PAGE and fluorography. The forms of cathepsin D are labeled as follows: P, proenzyme; I, endosomal intermediate; M, mature lysosomal enzyme.

Fig. 6. Morphology of endosomes, lysosomes and Golgi membranes is similar in Beclin KD cells compared with controls. Control or Beclin KD cells were seeded in parallel dishes at the same density and examined by immunofluorescence microscopy after 2 days, using the primary antibodies indicated at the left of the figure. The scale bar represents 20 μm.

Fig. 7. Suppression of Beclin expression does not interfere with endocytosis of a fluid phase marker, horseradish peroxidase (HRP) (A) Control (closed square) and Beclin KD cells (open circle) were seeded at the same density, grown for two days and then incubated for the indicated periods of time with 2 mg/ml HRP in DMEM + 1% BSA. Washed cells were lysed and HRP activity was determined as described in the Methods. Each point represents the mean ± S.E. from three determinations on parallel cultures. Similar results were obtained when the experiment was repeated with different batches of control and Beclin KD cells derived from separate retroviral infections and puromycin selections.

Fig. 8. Suppression of Beclin expression does not disrupt EGF-stimulated endocytosis or post-endocytic degradation of the EGF receptor. (A) Control or Beclin KD cells were fixed and processed for immunofluorescence detection of EGFR after overnight growth in serum-free medium (No EGF), and after 30 min or 70 min incubation with 200 ng/ml EGF. Scale bar = 10 μm. (B) Cells were harvested at the indicated times after addition of EGF and subjected to immunoblot analysis for total EGFR (upper panel). The bar graph (lower panel) shows the data derived from Kodak Imager scans performed on blots from three cultures harvested at each time point.

Fig. 9. Suppression of Beclin expression does not affect the growth rate of U251 cells. Control (solid line) and Beclin KD (dashed line) cells were seeded in 60-mm dishes on day-0 at an initial density of 200,000 cells/dish. On each of the indicated days cells were harvested from three dishes in each group and counted with Coulter Z1 particle counter (mean ± S.E.)

Fig. 1

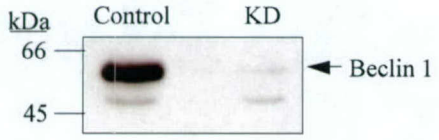

Fig. 2

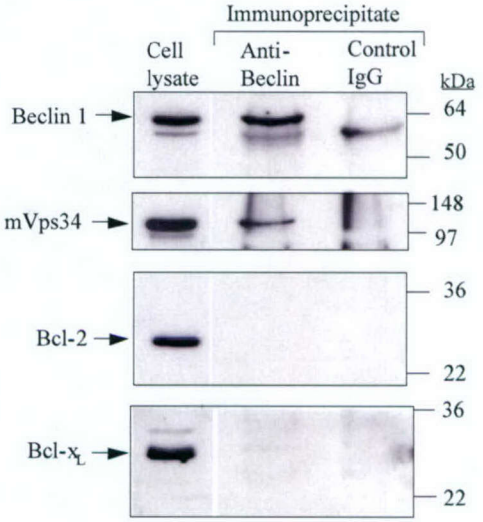

Fig. 3

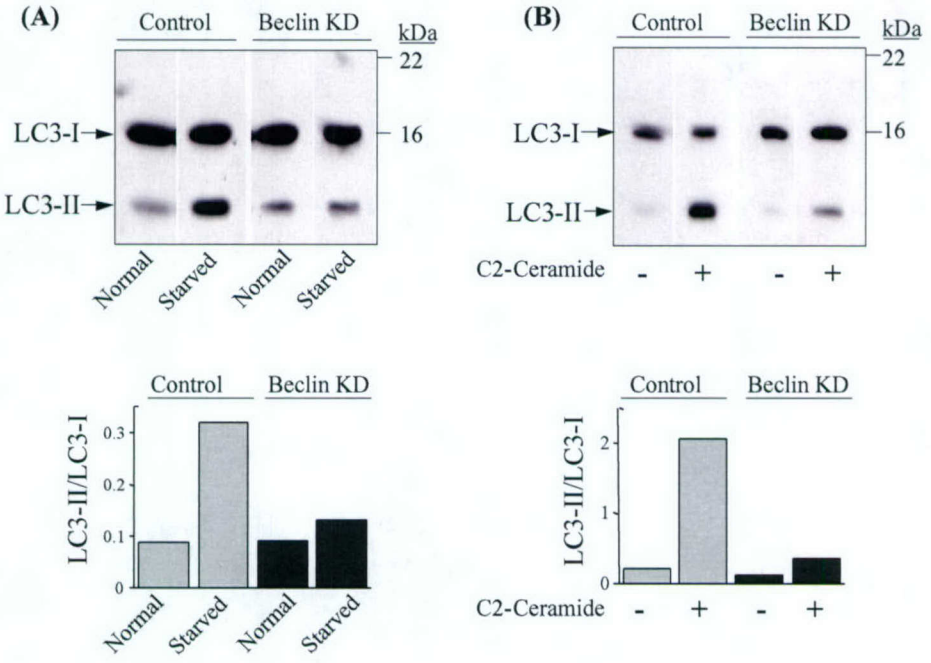

Fig. 4

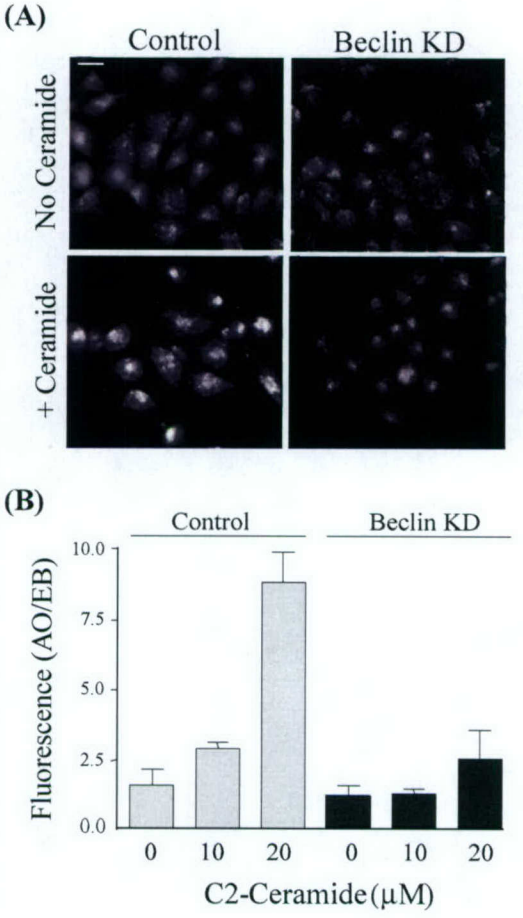
(A)
Control
Beclin KD
No Ceramide
+ Ceramide
(B)
Control
Beclin KD
Fluorescence (AO/EB)
10.0
7.5
5.0
2.5
0.0
0
10
20
0
10
20
C2-Ceramide (μM)

Fig. 5

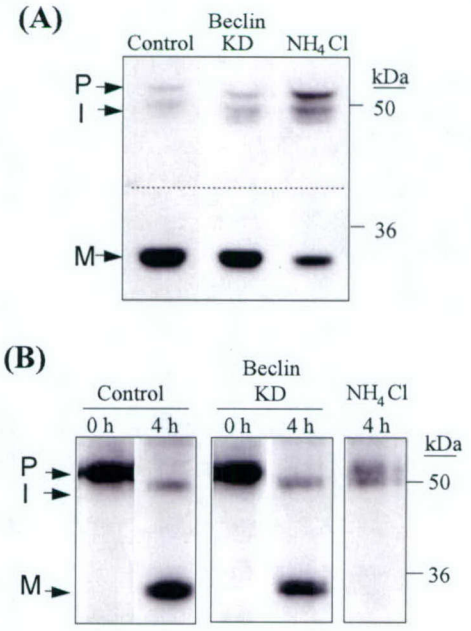
(A)
Control
Beclin KD
NH4Cl
kDa
P
I
M
50
36
(B)
Control
Beclin KD
NH4Cl
0 h
4 h
0 h
4 h
4 h
kDa
P
I
M
50
36

Fig. 6

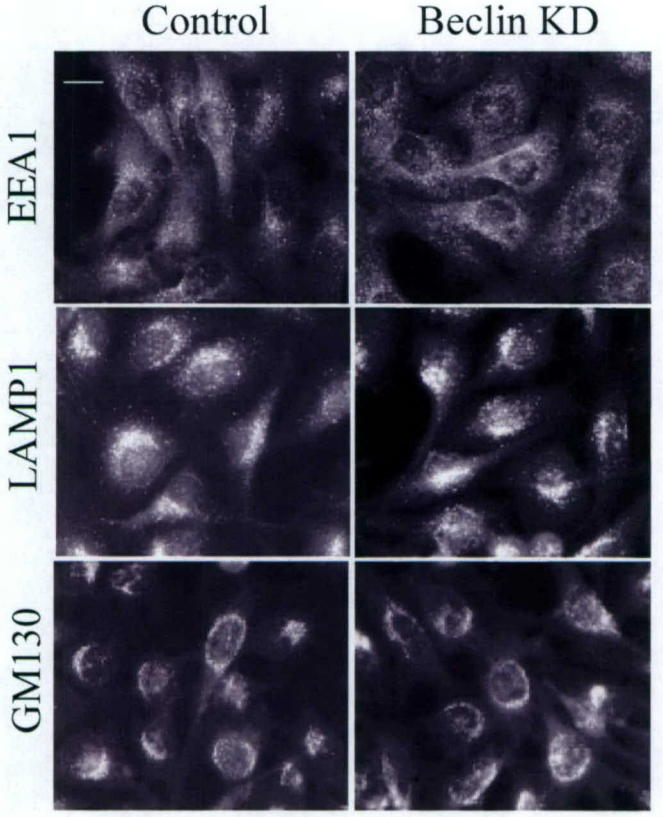
Control
Beclin KD
EEA1
LAMP1
GM130

Fig. 7

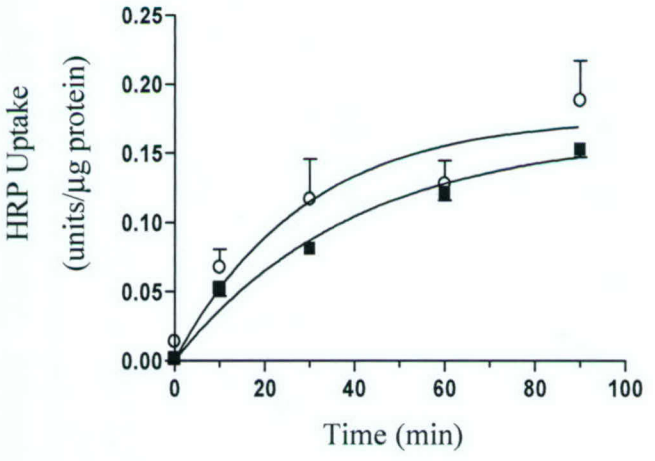
HRP Uptake
(units/µg protein)
0.25
0.20
0.15
0.10
0.05
0.00
0
20
40
60
80
100
Time (min)

Fig. 8

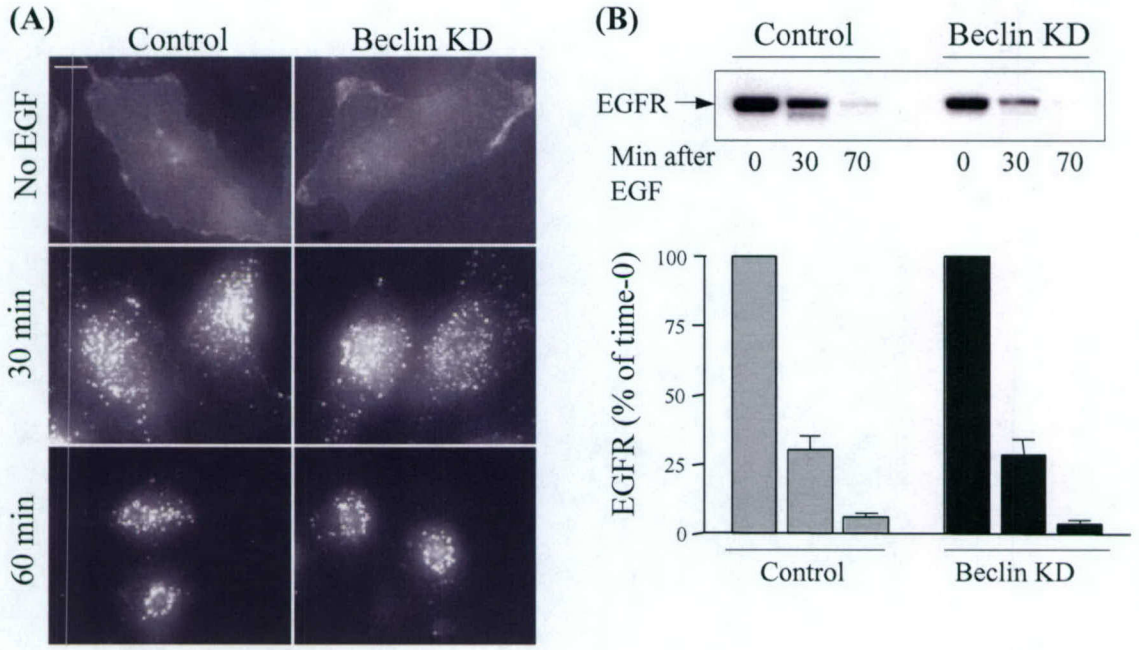
(A)
Control
Beclin KD
No EGF
30 min
60 min
(B)
Control
Beclin KD
EGFR
Min after EGF
0 30 70 0 30 70
EGFR (% of time-0)
100
75
50
25
0
Control
Beclin KD

Fig. 9

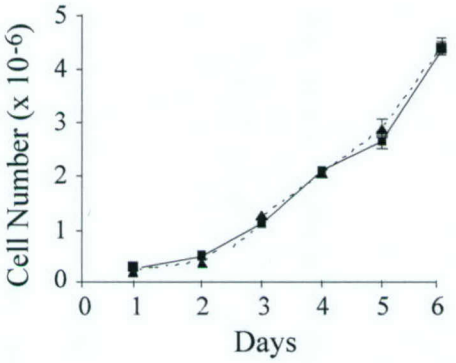
Cell Number (x 10-6)
5
4
3
2
1
0
0 1 2 3 4 5 6
Days

APPENDIX 2

Specific Function of Mammalian Vps34 Phosphatidylinositol 3-Kinase in Late *versus* Early Endosomes Revealed by siRNA-Mediated Gene Silencing

Erin E. Johnson, Jean H. Overmeyer, William T. Gunning and William A. Maltese

Department of Biochemistry and Cancer Biology, Medical University of Ohio,
Toledo, OH 43614, USA

Keywords: Endosome, Vps34, Phosphatidylinositol 3-kinase, Trafficking, Golgi, Lysosome

Abstract

The human class III phosphatidylinositol 3-kinase (PI3K), hVps34, converts phosphatidylinositol (PI) to phosphatidylinositol 3-phosphate, PI(3)P. Studies using inhibitors of PI3Ks have indicated that production of PI(3)P is important for a variety of vesicle-mediated trafficking events, including endocytosis, sorting of receptors in multivesicular endosomes, and transport of lysosomal enzymes from the *trans*-Golgi network (TGN) to the endosomes and lysosomes. This study utilizes siRNA-mediated gene silencing to define the specific trafficking pathways in which hVps34 functions in human U-251 glioblastoma cells. Suppression of Vps34 expression reduced the cellular growth rate and caused a striking accumulation of large acidic phase-lucent vacuoles that contain lysosomal membrane proteins, LAMP1 and LGP85. Analysis of these structures by electron microscopy suggests that they represent swollen multivesicular/late endosomes that have lost the capacity for inward vesiculation but retain the capacity to fuse with lysosomes. In contrast to the effects on late endosomes, suppression of hVps34 expression did not inhibit trafficking of cathepsin D from the TGN to late endosomes, endocytic uptake of fluid-phase markers, degradation of activated EGF-receptor, or association of a PI(3)P-binding protein, EEA1, with early endosomes. Nevertheless, EGF-receptor phosphorylation and signaling to ERK1/2 were enhanced in the absence of hVps34, consistent with the retention of the EGF-receptor on the limiting membranes of the enlarged late endosomes prior to degradation. Overall these findings indicate that hVps34 plays a major role in generating PI(3)P for internal vesicle formation in multivesicular/late endosomes and that, unexpectedly, other wortmannin-sensitive kinases or polyphosphoinositide phosphatases may be able to compensate for the loss of hVps34 and maintain PI(3)P levels required for vesicular trafficking in the early endocytic pathway or the TGN.

Introduction

Mammalian cells contain three distinct classes of phosphatidylinositol 3-OH kinases (PI3K's) [1,2]. The class III PI3K catalyzes the phosphorylation of phosphatidylinositol (PI) at the D-3 position of the inositol ring, generating phosphatidylinositol 3'-phosphate; PI(3)P [3]. The prototype for this class of enzyme, Vps34, was first identified in *Saccharomyces cerevisiae*, where it is one of several gene products required for delivery of soluble proteins to the vacuole [4,5] and for autophagic sequestration of cytoplasmic proteins during starvation [6,7]. Under both circumstances, association of Vps34 with cellular membranes depends on a myristoylated regulatory subunit, Vps15 [6,8]. In mammalian cells, Vps34 interacts with p150, a regulatory subunit similar to Vps15 [9].

Phosphatidylinositol 3'-phosphate is required for membrane recruitment of a number of proteins implicated in the regulation of vesicular transport and intracellular protein sorting [10,11]. Some of these proteins (*e.g.*, sorting nexins) contain a PX phosphoinositide binding domain [12-15], while others contain a structural motif termed the FYVE domain which binds to PI(3)P with high affinity [16-18]. Specific FYVE-domain proteins (EEA1, Rabenosyn-5, Rabip4) interact with Rab GTPases that control vesicle docking and fusion in the early endocytic pathway [19-22]. Interestingly, some Rabs that function in the early (Rab5) and late (Rab7) steps of the endocytic pathway also interact with the p150 subunit of the mammalian Vps34 complex, suggesting that the synthesis of PI(3)P and the recruitment of FYVE-domain proteins may be coordinately regulated [23,24].

Early evidence that PI3K's are important for protein trafficking in mammalian cells came from studies in which inhibitors of PI3K (wortmannin and LY294002) were found to impair targeting of procathepsin D from the *trans*-Golgi network (TGN) to the lysosomal compartment [25,26]. Subsequent work using a kinase-deficient dominant-negative form of mammalian Vps34 suggested that the block in cathepsin D maturation was indeed related to a requirement for the class III PI3K [27]. Separate lines of evidence have suggested that mammalian Vps34 PI3K may also be required for receptor sorting in the early endocytic pathway. For example, Siddhanta *et al.* [28] reported that

microinjection of an inhibitory antibody against Vps34 interfered with ligand-stimulated translocation of the PDGF receptor between peripheral early endosomes and perinuclear late endosomal compartments. Further investigations using inhibitory antibodies or wortmannin, have suggested that Vps34 may play an essential role in the formation of internal vesicles within multivesicular endosomes (MVE's) [29], a key sorting compartment between early endosomes and lysosomes (reviewed in [30]). Finally, in accord with studies in yeast, the mammalian Vps34 appears to play an important role in the process of macroautophagy in human cells subjected to nutrient deprivation [31].

Although the aforementioned experimental approaches have provided important insights into the functions of Vps34 in mammalian cells, each has particular limitations. For example, wortmannin can simultaneously inhibit multiple classes of PI3K [2] and at least one type of phosphatidylinositol 4-kinase [32], making it difficult to attribute physiological effects to a specific enzyme. Likewise, over-expression of interfering Vps34 mutants may tie up key effectors or docking proteins that normally interact with more than one distinct kinase. Finally, antibody microinjection studies, although precise, can be applied only to small populations of cells, precluding most biochemical analyses of protein trafficking pathways. In recent years the rapid development of methods for stable gene-silencing by RNA-interference (RNAi) has provided a powerful new option for defining the functions of specific proteins in mammalian cells [33-35].

In the present study we have applied siRNA technology to pinpoint the function of humanVps34 (hVps34) in cultured U-251 glioblastoma cells. Suppression of hVps34 caused extreme swelling of late endosomes, consistent with defective membrane internalization into MVEs without concomitant reduction of incoming membrane traffic from the TGN and early endosomes. However, in contrast to some earlier findings based on PI3K inhibitors, specific silencing of hVps34 expression did not impair: a) the exit of procathepsin D from the TGN, b) the endocytic internalization of cell surface receptors and fluid-phase markers, or c) the association of a FYVE-domain protein (EEA1) with early endosomes. These studies indicate that the role of hVps34 in producing PI(3)P for membrane

trafficking is limited mainly to the multivesicular late endosome compartments, and that other mechanisms may exist to produce PI(3)P required for vesicular trafficking in the early endosomes and *trans*-Golgi network.

MATERIALS AND METHODS

hVps34 gene silencing

U-251 human glioblastoma cells were obtained from the National Cancer Institute Frederick Cancer DCT Tumor Repository (Frederick, MD) and were maintained in Dulbecco's modified Eagle medium (DMEM), supplemented with 10% fetal bovine serum (FBS). The pSUPER.retro.puro vector was obtained from OligoEngine (Seattle, WA). A short hairpin RNA was designed to target a 19 bp sequence specific to human Vps34 mRNA. The oligonucleotide sequence used for siRNA interference with hVps34 expression corresponded to 5'-$_{675}$GTGTGATGATAAGGAATAT$_{693}$-3' of the human *VPS34* cDNA sequence (GenBank:BC033004), followed by a 9-nucleotide non-complimentary spacer (TTCAAGAGA) and the reverse compliment of the initial 19-nucleotide sequence. The control siRNA target sequence, 5'-$_{395}$AATACGGCATGTCTCGCCA$_{413}$-3', contained a one-base mismatch at position 407 from the *hVPS34* sequence and it did not match any other known sequences in the Genbank database. Retrovirus was produced in 293 GPG packaging cells [36] maintained in DMEM + 10% heat-inactivated FBS with 1 μg/ml puromycin, 300 μg/ml G418, and 2 μg/ml doxycycline. For transfection, the 293 GPG cells were seeded at $1.2x10^7$ cells/dish on 100 mm dishes in DMEM containing 10% heat inactivated FBS. Twenty-four hours later the cells were transfected with pSuper.retro.puro constructs using Lipofectamine-Plus reagent (Invitrogen, Carlsbad, CA). Forty-eight and seventy-two hours after transfection, the virus-enriched medium was collected and passed through a 0.22 μm filter. Infections of the U-251 cells were performed on three sequential days in the presence of 4.0 μg/ml hexadimethrine bromide (Sigma, St. Louis, MO). Cells were then

trypsinized and re-plated in selection medium containing 1 μg/ml puromycin. Following 5 days of selection, the surviving cells were pooled and utilized for studies described in the following sections.

For each experiment, control and hVps34 knockdown (KD) cell lines were harvested in order to verify the decrease in hVps34 expression. Briefly, equal amounts of protein were subjected to SDS-PAGE and immunoblot analysis using a polyclonal antibody against hVps34 (Zymed Laboratories, San Francisco, CA), followed by HRP-conjugated goat anti-rabbit IgG and ECL chemiluminescent detection reagent (Amersham-Pharmacia Biotech, Arlington Heights, IL) [37]. Immunoblot signals were quantified using a Kodak 440CF Image Station.

Characterization of vacuoles by immunofluorescence microscopy

Phase contrast images of control and hVps34 KD cells were obtained using an Olympus IX70 inverted microscope equipped with a digital camera, using SPOT imaging software (Diagnostic Instruments, Sterling Heights, MI). For immunofluorescence studies, cells were seeded on laminin-coated glass coverslips in 35mm dishes at 100,000 cells per dish. Twenty-four hours later, cells were washed with PBS, fixed with ice-cold methanol for 10 min, and blocked with 10% goat serum in PBS for 30 min. The following primary antibodies were applied for 1 h in PBS with 10% goat serum: anti-LAMP1 (University of Iowa Developmental Studies Hybridoma Bank, Iowa City, IA), anti-LGP85 (gift from Dr. Yoshitaka Tanaka), anti-M6PR and anti-calreticulin (Affinity Bioreagents, Golden, CO), anti-GM130 (BD Biosciences, San Diego, CA), and anti-LBPA (gift from Dr. Toshihide Kobayashi). Cells were washed three times with 10% goat serum in PBS, then incubated for 1 h with Alexa Fluor-568 goat anti-mouse (1:800, Molecular Probes, Eugene, OR) or Alexa Fluor- 488 goat anti-rabbit IgG (1:500, Molecular Probes, Eugene, OR) in PBS with 10% goat serum. After washing three times with PBS, the coverslips containing the cells were mounted with DAKO fluorescent mounting medium and photomicrographs were taken with a Nikon Eclipse 800 fluorescence microscope equipped with a Sensys digital camera. and ImagePro software (Media Cybernetics, Silver Spring, MD).

To visualize acidic intracellular compartments, cells were incubated with acridine orange (2.5 μg/ml; Molecular Probes, Eugene, OR) in serum-free, phenol red-free DMEM for 30 min at 37°C. Cells were then washed twice and the coverslips were then immediately inverted onto a drop of serum-free DMEM containing 20% glycerol and examined by fluorescence microscopy.

To highlight the endosomal and lysosomal compartments, cells were incubated with a fluid – phase tracer, Texas red-dextran (10,000MW, 500 μg/ml; Molecular Probes, Eugene, OR) in phenol red-free DMEM with 10% FBS for 16 h at 37°C. Following a 2 h incubation in dextran-free DMEM, cells were washed with PBS, fixed with ice-cold methanol, and stained with anti-LAMP1 followed by FITC-conjugated goat anti-mouse IgG (Sigma, St. Louis, MO).

Electron microscopy

For transmission electron microscopy (EM), cell pellets fixed with 3% glutaraldehyde (GA) for 1 h were washed three times for 10 min with 0.2 M sodium cacodylate, post-fixed for 2 h with 1% OsO_4 and incubated for 1 h with saturated uranyl acetate. Dehydration was carried out via a graded series of chilled ethanol solutions (30-100%) and a final dehydration with 100% acetone. Cells were infiltrated overnight in Spurr's resin (Electron Microscope Sciences, Fort Washington, PA) and ultrathin sections were obtained and collected on copper 300-mesh support grids. Sections were stained with uranyl acetate and lead citrate, and examined using a Philips CM 10 transmission electron microscope.

For immunogold staining of cathepsin D, cell pellets were fixed with 1% glutaraldehyde and washed sequentially with cacodylate buffer and 50 mM M ammonium chloride. Following dehydration with ethanol only, the cells were infiltrated and embedded in LR White® embedding media (London Resin Co., Ltd., Berkshire, England). Sections were collected with gold support grids and blocked with a solution of 10% fish gelatin in PBS for 1 h and incubated for 2 h with goat anti-cathepsin D antibody (Santa Cruz Biotechnology, Santa Cruz, CA) (1:40 dilution in PBS) followed by 1 h with donkey anti-goat IgG conjugated with 6 nm colloidal gold (Jackson ImmunoResearch Labs,

West Grove, PA). The samples were post-fixed with 1% glutaraldehyde, washed, and stained with uranyl acetate and lead citrate.

For peroxidase staining, the cell pellets were fixed with GA and OsO_4, washed as above, and resuspended in DAB reaction medium (0.5 M Tris pH 7.6, 1 mg/ml 3,3-diaminobenzidine-HCl, 0.01% hydrogen peroxide) overnight. Pellets were then washed 3 times with cacodylate buffer and processed for routine EM as described above with the exclusion of any steps requiring uranyl acetate.

Metabolic labeling and immunoprecipitation of cathepsin D

Cells were seeded in 100 mm dishes at 350,000 cells per dish in medium containing 1 μg/ml puromycin. After 24 h the cells were washed and incubated for 30 min in methionine-free DMEM containing 10% FBS. The cultures were then labeled for 30 min in the same medium containing 100 μCi/ml ^{35}S-methionine/cysteine (Easy Tag™ EXPRESS, 1.18 μCi/mmol, NEN/PerkinElmer, Boston, MA), washed once with PBS, and then chased in complete medium supplemented with 200 μM methionine and 200 μM cysteine for 4 h. At the end of the chase, cells were washed twice, scraped into ice-cold PBS, and collected by centrifugation for 5 min at 400 x g . Cell lysates were prepared in 200 μl RIPA buffer (100 mM Tris-HCl, pH, 7.4, 2 mM EDTA, 0.5% Nonidet P-40, 0.1 % SDS, 0.5% sodium deoxycholate) supplemented with complete mini protease inhibitors (Roche, Indianapolis, IN). Insoluble material was removed by centrifugation at 100,000 x g for 1 h at 4°C and the soluble fractions were pre-cleared by incubation with protein A sepharose beads for 30 min at 4°C. After removal of the beads, immunoprecipitation was performed essentially as previously described [39], using a polyclonal antibody against cathepsin D (Biodesign International, Saco, ME). SDS-PAGE and fluorographic analysis of the immunoprecipitated proteins was performed by standard methods [40].

Endocytosis of horseradish peroxidase (HRP)

Cells were washed with DMEM and incubated with 2 mg/ml HRP (Sigma, St. Louis, MO) in DMEM containing 1% BSA at 37°C. At the time points indicated in Fig. 6, cells were placed on ice, washed three times with ice-cold PBS containing 1% BSA and one time with PBS alone. Cells were then scraped from the dish into PBS, pelleted by centrifugation, washed once more with PBS and then disrupted in PBS containing 0.5% Triton X-100. Cell lysates were clarified by centrifugation at 10,000 x g for 5 min at 4°C and HRP activity in the supernatant was determined using a Turbo TMB enzyme-linked immunosorbent assay kit (Pierce Chemical, Rockford, IL). Results were normalized to protein, measured with a BCA protein assay kit (Pierce Chemical, Rockford, IL).

Epidermal growth factor receptor (EGFR) internalization and degradation

Cells infected with the hVps34 KD and control vectors were selected for 5 days and then seeded at equal density in 60 mm dishes. On the following day, the cells were switched to serum-free medium and maintained for 16 h to allow the EGFR to accumulate on the cell surface. Receptor internalization and degradation were then stimulated by addition of EGF (100 ng/ml, Upstate Biotechnology, Lake Placid, NY). At 0, 30 and 60 min after addition of EGF, cells were washed twice with ice-cold PBS and harvested in SDS-PAGE sample buffer. Equal amounts of protein were then subjected to SDS-PAGE and immunoblot analysis, using antibodies against total EGFR (BD Biosciences, San Diego, CA), phospho-EGFR (Cell Signaling Technology, Beverly, MA), phospho-ERK and total ERK (Cell Signaling Technology, Beverly, MA). Chemiluminescence (ECL) signals were quantified as described above.

Subcellular distribution of EEA1

Cells were trypsinized and collected by centrifugation at 400 x g for 5 min at 4°C. Cell pellets were washed 3 times with ice-cold PBS and allowed to swell for 15 min at 4°C in hypotonic buffer (10 mM HEPES, pH 7.5, 1.5 mM $MgCl_2$, 10 mM KCl, and 1 mM DTT and protease inhibitors). The cells

were disrupted with 15 strokes of a Teflon homogenizer and sucrose was added to a final concentration of 0.25 M. Soluble and particulate fractions were obtained by centrifugation at 100,000 x g for 1 h at 4°C. Equal percentages of the soluble and particulate fractions were then subjected to SDS-PAGE and immunoblot analysis using an antibody against EEA1 (BD Biosciences, San Diego, CA). Chemiluminescence signals were quantified as described earlier. For immunofluorescent localization of EEA1, cells were fixed with 3% paraformaldehyde for 15 min at room temperature, quenched with 50 mM NH_4Cl in PBS (5 min), permeabilized with 50 μg/ml digitonin in PBS (5 min), and blocked with 10% goat serum in PBS for 30 min. Anti-EEA1 was then applied for 1 hr followed by Alexa Flour-568 goat anti-mouse (1:800, Molecular Probes, Eugene, OR).

Cell growth and survival

To assess cell growth, hVps34 KD or control cells that had been selected for two days were seeded in 35mm dishes at 50,000 cells per dish. On the days indicated in Fig. 10A, the cells were trypsinized and counted using a Coulter Z-series particle counter (Beckman-Coulter Corporation, Fullerton, CA). To measure DNA synthesis, cells were seeded in 25 cm^2 flasks at 150,000 cells per flask. On days 2 and 6, cells were incubated for 5 h in medium containing 1 μCi/ml [methyl-^{3}H]-thymidine (5 Ci/mmol, Amersham Biosciences, Piscataway, NJ). Incorporation of radioactivity into TCA-precipitable material was determined as described previously [38].

For assessment of apoptotic cell death, cells were seeded in 60 mm dishes at 200,000 cells per dish. On days 2 and 6, floating and adherent cells were harvested and stained with annexin-V and 7-amino-actinomycin D as described in the protocol for the Guava Nexin™ kit (Guava Technologies Inc., Hayward, CA). Staining was quantified using a Guava personal cytometer. Control cells treated for 18 h with 10 ng/ml TNFα (Calbiochem, San Diego, CA) plus 2.5 μg/ml cyclohexamide (Sigma, St. Louis, MO) served as a positive control for apoptosis.

RESULTS

Reduction of hVps34 expression by siRNA-mediated gene silencing causes accumulation of cytoplasmic vacuoles

To obtain a cell population in which expression of hVps34 was specifically and uniformly suppressed, we utilized a replication-deficient retroviral vector that drives the expression of RNAi sequences and confers puromycin resistance on infected cells [35]. Vectors were engineered to contain either a sequence matching a unique region of the hVPS34 mRNA, or a "control" sequence that did not match any known GenBank entry. In preliminary tests with several cell lines infected with a GFP reporter construct, the human U-251 glioblastoma line showed high initial infection efficiency with the retroviral vector. Therefore, we chose to use this cell line for studies of hVps34. As illustrated by the immunoblots in Fig. 1A, expression of hVps34 was almost undetectable in puromycin-resistant cells that received the hVps34 "knockdown" vector (KD), compared with cells that were infected with the control vector. In all of the experiments described in this paper, similar immunoblot results were obtained, verifying that expression of hVps34 was decreased by at least 90% relative to the parallel control cultures. Expression levels of several unrelated proteins (e.g., lactate dehydrogenase, calreticulin, lamin B) were comparable in the control and KD cells, indicating that the loss of hVps34 expression was not due to a general effect of the siRNA on protein synthesis.

Examination of the cultures by phase contrast microcopy revealed striking morphological differences between the hVps34 KD cells and the matched controls (Fig. 1B). Specifically, the KD cells were filled with numerous large phase-lucent spherical cytoplasmic vacuoles ranging between 1 and 8 microns in diameter. Electron microscopy revealed that the vacuoles were generally electron lucent (Fig. 2A), although some contained sparsely distributed electron-dense material along with a few internal vesicles or membrane whorls (Fig. 2B). The vacuoles were circumscribed by a single membrane, indicating that they did not represent enlarged autophagosomes (Fig. 2B).

Vacuoles in hVps34 KD cells are derived from late endosomes

Previous reports have suggested that hVps34 is associated with Golgi [41] and endosomal [23] membranes in mammalian cells. To begin to assess the origin of the vacuoles in the hVps34 KD cells, we performed indirect immunofluorescence microscopy using a series of antibodies against proteins localized in specific organelles (Fig. 3). The limiting membranes of the vacuoles were clearly outlined by antibodies against LAMP1 and another late endosome/lysosome glycoprotein, LGP85 [42]. The enlarged vacuoles in the hVps34 KD cells did not react with an antibody against lysobisphosphatidic acid (LBPA), a phospholipid that is normally concentrated in the internal membranes of MVEs and late endosomes [43]. In the control cells, LAMP1, LGP85 and LBPA were all localized to clusters of punctuate structures adjacent to the nucleus, typical of the late endosome and/or lysosome distribution of these markers seen in many types of cells.

Immunofluorescent staining with antibodies to proteins associated with membranes of endoplasmic reticulum or Golgi apparatus confirmed that the vacuoles did not arise directly from these compartments in the hVps34 KD cells (Fig. 3). Calreticulin exhibited a diffuse pattern throughout the cytoplasmic regions not occupied by the vacuoles, and GM130 exhibited a compact juxtanuclear distribution typical of Golgi localization. The cation-independent mannose-6-phosphate receptor (M6PR) did not accumulate in the limiting membranes of the vacuoles. Instead, M6PR was detected mainly in a compact region adjacent to the nucleus, similar to the GM130 Golgi marker. The M6PR is involved in the delivery of newly synthesized lysosomal hydrolases from the TGN to multivesicular endosomes [44-46]. The distribution of M6PR in the control and hVps34 KD cells is consistent with previous reports indicating that at steady state most of the M6PR is localized in the TGN [43,47].

To further characterize the cytoplasmic vacuoles, we performed supravital staining of the cells with the lysosomotropic agent, acridine orange (AO) (Fig. 4A). The non-protonated monomeric form of AO emits green fluorescence in the cytoplasm. However, when the dye enters an acidic

compartment (*e.g.*, lysosomes or late endosomes), the protonated form becomes trapped in aggregates that fluoresce bright red or orange [48-50]. The images in Fig. 4A demonstrate that the numerous vacuoles observed in the hVps34 KD cells are acidic vesicular organelles that sequester AO.

Based on the presence of lysosomal membrane markers and their ability to sequester AO, we hypothesized that the vacuoles in the hVps34 KD cells were derived from late endosomes or lysosomes. To further test this hypothesis, we labeled the endosomal system by adding a fluid phase tracer, TxR-dextran, to the culture medium for 16 h (Fig. 4B). The distribution of TxR-dextran was compared with that of LAMP1, a membrane glycoprotein restricted to lysosomes and late endosomes [51]. In the control cells the TxR-dextran was concentrated in a cluster of small vesicles adjacent to the nucleus. Consistent with the expected uptake of TxR-dextran into endosomes and lysosomes, the tracer showed extensive co-localization with LAMP1-positive compartments (Fig. 4B). Examination of the hVps34 KD cells revealed that the fluid phase tracer was incorporated into some of the large LAMP1-positive cytoplasmic vacuoles (arrows) as well as numerous smaller vesicular structures (Fig. 4B). However, the persistence of some LAMP1-positive vacuoles that did not incorporate TxR-dextran after prolonged incubation (arrow heads) suggests that a subpopulation of these structures may be functionally disengaged from the fluid-phase endocytic pathway.

Suppression of hVps34 expression does not disrupt the PI(3)P-dependent localization of the early endosome protein, EEA1

In an attempt to assess the morphology of the early endosomes, we examined the subcellular distribution of Early Endosomal Antigen 1 (EEA1), a FYVE-domain protein that is known to be recruited to the early endosome membrane in a PI(3)P and Rab5 dependent manner [20,52]. There was no clear association of EEA1 with the membranes of the numerous large vacuoles in the hVps34 KD cells (Fig. 5A). Instead, the protein was detected predominantly in a population of smaller vesicles with a pattern similar to the control cells. In careful comparisons of the EEA1-positive compartments

in control *versus* hVps34 KD cells, we occasionally observed ring-like structures that could represent swollen early endosomes in the KD cells (Fig. 5A, arrow). However, these structures were distinct from the more abundant and much larger phase-lucent vacuoles. In contrast to the bright punctate fluorescence pattern of EEA1 in the control and hVps34 KD cells, cells treated with 1 μM wortmannin for 1 h showed only a diffuse reticular staining pattern, consistent with the release of EEA1 from endosomal membranes reported to occur in cells treated with PI3K inhibitors [20,53].

To further examine the subcellular distribution of EEA1, control and KD cells were fractionated into cytosolic and particulate components and the partitioning of EEA1 between these components was determined by immunoblot analysis (Fig. 5B). The results revealed a very similar distribution of EEA1 in the control and hVps34 KD cells, with approximately 21-24% of the total EEA1 in the particulate fraction. In contrast, a 1-h treatment with 1 μM wortmannin resulted in an easily detected decline in the proportion of EEA1 associated with the particulate fraction (12%). When considered together with the immunofluorescence localization studies in Fig. 5A, these results indicate that EEA1 is able to associate with endosomal membranes in U-251 cells under conditions where expression of hVps34 is almost completely suppressed.

Endocytic internalization of HRP and degradation of the epidermal growth factor receptor (EGFR) are not blocked in hVps34 KD cells

The preceding studies of EEA1, coupled with the earlier observation that a fluid-phase tracer, TxR-dextran, was incorporated into LAMP1-positive compartments in the hVps34 KD cells (Fig. 4B) suggested that production of PI(3)P by hVps34 was not essential for delivery of early endosome cargo to late endosomes in U-251 cells. Previous studies have shown that when vesicular transport from early endosomes to late endosomes is inhibited, there is a reduction in cellular uptake of the soluble endocytic tracer, HRP [54,55]. Thus, to further explore the integrity of the early endocytic pathway in the hVps34 KD cells, we determined the kinetics of HRP uptake. As shown in Fig. 6, the rate of HRP

uptake was not reduced in the KD cells. On the contrary, HRP uptake was significantly increased compared with the controls. Although the basis for this increase remains to be determined, it clearly argues against hVps34 being required for early steps in the endocytic internalization of HRP.

As a final means to evaluate protein trafficking in the endocytic pathway, we examined the fate of activated EGFR. In serum-deprived cells grown in the absence of EGF, degradation of EGFR is minimal and receptors accumulate on the cell surface. However, upon addition of EGF, the receptors are rapidly activated by tyrosine phosphorylation in the C-terminal cytoplasmic domain and the EGF-EGFR complexes are internalized into clathrin-coated early endosomes. Down-regulation of activated receptors depends upon their delivery to multivesicular endosomes, where receptor complexes are sorted into internal vesicles that are ultimately degraded when late endosomes fuse with lysosomes [56]. When EGFR was localized by immunofluorescence 30 min after addition of EGF to hVps34 KD cells, most of the receptors were found in small internal vesicles that were distinct from the large vacuoles labeled by the late endosome/lysosome marker, LGP85 (Fig. 7A). However, after 60 min, some EGFR could be detected in the limiting membranes surrounding the large LGP85-positive vacuoles (Fig. 7A, arrows). This suggested that delivery of EGFR from early endosomes to the surface membranes of the enlarged late endosomal structures was not impaired in the hVps34 KD cells.

To examine degradation of the EGFR, immunoblot analysis of total EGFR was performed at intervals after addition of EGF. The results indicate that overall degradation of the receptor was similar in the hVps34 KD cells compared with the controls (Fig. 7B). To assess the amount of activated receptor at intervals after EGF stimulation, the blots were re-probed with an antibody that specifically recognizes phosphorylated Y^{1068} in the C-terminal domain of the receptor. The C-terminal domain faces the cytoplasm when EGFR is in the limiting membrane of the endosome, but it is incorporated into the lumen of vesicles that invaginate to the interior of the MVE [56]. As shown in Fig. 7C, nearly all of the EGFR was in the non-phosphorylated state at the starting point, but within 30 min of adding EGF both control and hVps34 KD cells exhibited a dramatic increase in the proportion

of phospho-EGFR relative to total receptor. Interestingly, although there was little difference in the overall degradation of EGFR (Fig. 7B), the ratio of phospho-EGFR to total EGFR in the hVps34 KD cells was approximately double that observed in the control cells (Fig. 7C). Thus, it appears that prior to being exposed to lysosomal proteases, a higher percentage of the EGFR remains phosphorylated in the hVps34 KD cells. In accord with this concept, activation of the ERK (p44/42 MAP Kinase) signaling pathway, as measured by the ratio of phospho-ERK1/2 to total ERK1/2, was augmented in the hVps34 KD cells compared with the controls (Fig. 7D).

Silencing of hVps34expression allows transport of procathepsin D from the TGN to endosomes, but slows proteolytic processing of the endosomal intermediate

To determine if the enlarged endosomal structures in the hVps34 KD cells were capable of accepting cargo normally delivered to late endosomes from the TGN, we focused on the lysosomal enzyme, cathepsin D [57]. Newly synthesized procathepsin D (51-53 kDa) associates with the cation-independent M6PR in the TGN and is delivered to the endosomal compartment, where it is activated by removal of the pro-peptide to generate an intermediate that migrates at 46-48 kD on SDS gels. The final step in cathepsin D processing is completed in the lysosomes, where the intermediate is cleaved to the mature form, which contains two non-covalently linked chains of 31 kDa and 14 kDa [58,59].

To evaluate the processing of newly synthesized procathepsin D, we performed a pulse-chase analysis (Fig. 8A). When ^{35}S-methionine-labeled cathepsin D was immunoprecipitated after a 30 min pulse, nearly all of the radiolabeled protein was in the 53 kDa form in both control and KD cells. After a 4 h chase, the control cells converted most of the procathepsin D to the mature form, with some intermediate form still detected. There was no residual radiolabeled procathepsin D in the hVps34 KD cell after a 4 h chase, suggesting that delivery of procathepsin D to the late endosome compartment was not substantially altered in the absence of hVps34 (Fig. 8A). However, compared with the control, there was a 50% decrease in the relative amount of the mature 31 kDa cathepsin D and a corresponding

increase in the 47 kDa intermediate (Fig. 8A). In contrast, a complete block instituted by raising the endosomal and lysosome pH with NH_4Cl is manifested by the absence of any radiolabeled 31 kDa cathepsin D after a 4 h chase (Fig. 8A). These results are indicative of a kinetic block at the late endosome to lysosome transition, resulting in slower lysosomal processing of the cathepsin D intermediate.

This interpretation is reinforced by the immunoblot depicted in Fig. 8B, which shows that the steady-state level of the 47 kDa cathepsin D intermediate was markedly elevated in the hVps34 KD cells. On the other hand, in agreement with the pulse-chase study, there was no accumulation of the 53 kDa procathepsin D that could indicate a problem with trafficking from the TGN. Likewise, immunoblot analysis of procathepsin D released into the medium showed no indication that an increased amount of procathepsin D was being diverted into the secretory pathway in the hVps34 KD cultures (not shown). The similar levels of mature cathepsin D in the control and KD cells might seem puzzling at first, given the slower intermediate processing observed in Fig. 8A. However, this is most likely related to the fact that lysosomal enzymes have long half-lives compared with their precursors [60-62] so that, over time, a reduced rate of intermediate processing might have an imperceptible impact on the accumulated pool of end product detected by immunoblot assay.

The finding that final proteolytic processing of the 47 kDa cathepsin D intermediate was slowed but not completely blocked in the hVps34 KD cells, suggested that the enlarged endosomes might be able to acquire lysosomal characteristics by limited fusion with pre-existing lysosomes. To investigate this possibility, we examined the hVps34 KD cells by electron microscopy after staining them for endogenous lysosomal peroxidase activity with 3,3-diaminobenazidine (DAB) (Fig. 9A). Distinct spherical DAB-positive lysosomes were observed throughout the cytoplasmic compartment, contrasting with the larger DAB-negative vacuolar structures. In many instances the DAB-positive lysosomes were in direct contact with the enlarged endosomes (Fig. 9A, arrows), and in some cases these structures appeared to have merged, releasing peroxidase-positive material into the lumen of the

vacuoles (Fig. 9A, arrowheads). The hVps34 KD cells were also subjected immuno-gold electron microscopy, using a primary antibody against cathepsin D to identify lysosomes (Fig. 9B). We frequently noted smaller electron-dense structures heavily labeled with gold particles in close proximity to the larger electron-lucent vacuoles (Fig. 9B, arrow), and in some cases it appeared that cathepsin D was being delivered to the lumen of the vacuole after fusion with the structure (Fig. 9B arrowhead). These findings indicate that the enlarged endosome-derived vacuoles in the hVps34 KD cells retain the capacity to fuse with lysosomal compartments.

Suppression of hVps34 expression inhibits cell proliferation

The cells in the hVps34 KD cultures were approximately 2-3 times larger than those in the controls, and they did not reach a comparable density when maintained for several days after the initial puromycin selection. This prompted us to ask whether suppressing the expression of hVps34 might affect the growth of the U-251 cells. As shown in Fig. 10A, the growth rate of the KD cells was markedly reduced compared to the matched control cell line. A decreased rate of cell proliferation was confirmed by comparing the incorporation of ^{3}H-thymidine into DNA in control *versus* KD cells at points where the control cells were at low density (day-2) or near confluency (day-6). (Fig. 10B). Apoptotic cell death, measured by annexin staining, was not a major factor in reducing the density of hVps34 KD cells, even though U-251 cells were capable of a robust apoptotic response when treated with TNFα (Fig. 10C).

Discussion

The present study is the first to use the highly specific method of siRNA-mediated gene-silencing to explore the function of the human class-III PI3K, hVps34. Our observations indicate that silencing of hVps34 expression mainly affects membrane-sorting events within the multivesicular and late endosome compartments, with surprisingly little or no effect on the export of proteins from the

TGN to endosomes or vesicular trafficking through the early part of the endocytic pathway. The acidic characteristics of the vacuoles in the hVps34 KD cells, coupled with the dearth of internal structures and the presence of LAMP1 and LGP85 in their limiting membranes, indicates that they represent enlarged late endosomes. Interestingly, despite their distorted size, these structures seem to retain a substantial capacity to merge with primary lysosomes, allowing for normal degradation of the EGFR and only partial impairment of the processing of the intermediate form of cathepsin D to the mature form.

One of the novel findings emerging from the present studies is the absence of any effect of blocking hVps34 expression on the first step in procathepsin D processing, which depends on transport of the proenzyme from the TGN to the late endosomes [58,59]. Previous reports have indicated that hVps34 is localized predominantly in Golgi membranes [41] and that inhibition of PI3K activity with wortmannin causes intracellular accumulation of unprocessed procathepsin D, which then enters the secretory pathway [25]. Follow-up studies by Row *et al.* [27] implicated Vps34 as the probable wortmannin target by showing that overexpression of a kinase-deficient form of rat Vps34 produced a similar impairment in procathepsin D conversion to the 47-48 kDa endosomal intermediate. The discrepancy between these earlier results and the present findings based on siRNA-mediated silencing of hVps34 could be related to differences in the mechanisms used for interference with hVps34 function. For instance, siRNA is expected to eliminate endogenous hVps34 and any PI(3)P normally produced by this enzyme at specific subcellular sites. On the other hand, overexpression of a kinase-deficient form of Vps34 may act by competing with endogenous hVps34 for binding to the p150 adapter [9] or other interacting proteins like Rab5 [23] or Rab7 [24]. This might cause perturbations of protein trafficking pathways due to titration of Vps34 partners, but not necessarily to loss of PI(3)P production by endogenous hVps34.

If hVps34 is not specifically responsible for producing PI(3)P needed for vesicular trafficking out of the TGN, it is conceivable that other closely related PI3Ks may fulfill this role. In this regard, it

is worth noting that two novel PI3K activities have been described in the TGN. Both appear to be required for genesis of constitutive transport vesicles. The first is associated with TGN38 and a regulatory complex termed $p62^{cplx}$ [63]. The second was found to associate with TGN46 [64]. Neither of these PI3Ks has yet been characterized in sufficient detail to know how closely they might be related to Vps34 or whether they might be required for endosome and lysosome-directed trafficking of proenzymes associated with the M6PR.

Our finding that hVps34 knockdown had no apparent effect on the subcellular distribution of the early endosome protein, EEA1, was unexpected since previous studies using FYVE-domain probes have demonstrated that PI(3)P is concentrated in microdomains in the membranes surrounding early endosomes, as well as in the internal vesicles of multivesicular endosomes [65,66]. Moreover, as mentioned earlier, inhibition of PI3K activity with wortmannin has been reported to cause the release of EEA1 from early endosomes [20,53]. Thus, our results raise the intriguing possibility that the role of hVps34 is restricted to producing PI(3)P for specific compartments such as the multivesicular endosome, while other kinases or phosphatases can generate PI(3)P in early endosomes. Although we can only speculate about the nature of such alternative pathways, several possibilities are worth considering: One possibility is that the class I or class II PI3Ks can contribute to maintaining the pool of PI(3)P in early endosomes. Class-I PI3Ks are heterodimers composed of p110 catalytic subunits and p85 or p55 regulatory subunits [2]. Although the large increase in cellular $PI(3,4,5)P_3$ typically observed upon stimulation of class I enzymes suggests that $PI(4,5)P_2$ is the preferred substrate *in vivo,* these enzymes can phosphorylate the 3-position of PI in cell-free systems [1,67]. Thus, the possibility that class-I PI3K can produce sufficient PI(3)P for vesicular transport in some compartments cannot be completely ruled out. The physiological function of the class II enzymes remains poorly understood, but there is some evidence that they are localized in the TGN and clathrin-coated vesicles [68]. It is indeed quite likely that the class II PI3Ks can produce PI(3)P in mammalian cells, since these enzymes preferentially phosphorylate PI over PI(4)P and $PI(4,5)P_3$ *in vitro* [1,69]. A final scenario worth

considering is the possibility that PI(3)P can be generated in specific subcellular compartments through the sequential actions of inositol polyphosphate 5-phosphatase [70] and inositol polyphosphate 4-phosphatase [71,72], which are capable of removing the 5'-phosphate and the 4'-phosphate from $PI(3,4,5)P_3$ and $PI(3,4)P_2$, respectively. Such a mechanism might be particularly relevant for preserving the PI(3)P pool in the early endosomes derived from regions of the plasma membrane where $PI(3,4,5)P_3$ appears to be generated [73].

There have been conflicting reports regarding the importance of PI3K for post-endocytic sorting of activated receptors that enter the cell *via* clathrin-coated pits. In one study, wortmannin inhibited the formation of internal vesicles in the MVEs of HEp2 cells, but the EGFR was still able to reach the perimeter membrane of lysosomes, exposing the N-terminal ligand-binding domain to a degradative environment [29]. However, in another study with BHK-21 cells [53], wortmannin treatment prevented the translocation of ligand-stimulated EGFR from early endosomes to late endosomes. Our results support the conclusion that hVps34 is not absolutely essential for translocation of activated EGFR to late endosomes (Fig. 7).

Within 60 min after EGF stimulation, the EGFR in the hVps34 KD cells reached the limiting membranes of enlarged LGP85-positive vacuoles and was degraded to an extent similar to that seen in the control cells. Since fusion of multivesicular late endosomes with lysosomes is required for EGFR degradation [74], our results indicate that the enlarged vacuoles generated in the absence of hVps34 retain the capacity for fusion with pre-existing lysosomes. This conclusion is further supported by the ultrastructural evidence, where some vacuoles appear to be merging with DAB-positive structures containing endogenous peroxidase activity or electron-dense structures that contain cathepsin D (Fig. 9). Interestingly, although overall degradation of the EGFR was not substantially different between control and hVps34 KD cells, a much higher proportion of the total EGFR remained in an active phosphorylated state capable of activating the ERK pathway (Fig. 7). One mechanism for dephosphorylation of the EGFR involves protein tyrosine phosphatase 1B on the surface of the

endoplasmic reticulum [75]. However, the possibility that tyrosine dephosphorylation may also occur in conjunction with internalization of the EGFR into the MVEs has also been suggested [76]. Since, the phosphorylated C-terminal domain of the EGFR on the surface of endosomes is capable of interacting with cytoplasmic adaptors and signaling to the ERK pathway [77,78], we conclude that in the absence of PI(3)P generated by hVps34, an increased proportion of the EGFR is retained on the surface of the enlarged endosomes in an active phosphorylated state prior to eventual degradation of the N-terminal domain by lysosomal proteases entering the lumen of the vacuole.

The morphological phenotype of the hVps34 KD cells resembles the "class E" vacuolar phenotype that can be triggered in mammalian cells by interfering with the assembly of the ESCRT-III complex on multivesicular endosomes [79,80]. This suggests a molecular mechanism whereby suppression of hVps34 might cause a failure of inward vesiculation of MVEs. Specifically, $PI(3,5)P_2$ has been identified as an important phospholipid for membrane recruitment of hVps24, a key component of ESCRT-III [81]. Since the kinase responsible for generating $PI(3,5)P_3$ is in fact a PI(3)P-binding FYVE-domain protein termed PIKfyve [82,83], silencing hVps34 and localized depletion of PI(3)P might prevent membrane recruitment of PIKfyve and the subsequent $PI(3,5)P_3$-dependent assembly of ESCRT-III. Further investigation of this possibility will have to await the development of antibodies that can detect endogenous PIKfyve, which is expressed at very low levels in most cells.

In addition to the striking morphological changes affecting the late endosome compartment, we noted a markedly reduced growth rate in the hVps34 KD cells. In an earlier study Siddhanta *et al.* [28] found that a neutralizing antibody against hVps34 could block the insulin-stimulated increase in DNA synthesis in GRC-LR+73 cells only when it was microinjected during a defined temporal window of the G1 phase of the cell cycle. This raises the intriguing possibility that, in addition to its role in membrane sorting in the multivesicular endosome, hVps34 might play a specific role in the control of DNA replication and/or transcription. Although this possibility remains to be explored in mammalian

cells, studies using plant cells have found that Vps34 is associated with discrete nuclear and nucleolar transcription sites [84,85]. In light of these observations, the prospect of a role for hVp34 in the nucleus of mammalian cells promises to be an important topic for future study.

Acknowledgements

This work was supported in part by grants from the NIH (RO1CA34569) and the U.S. DOD (Idea Award BC031231)

References

[1]. Fruman, D. A., Meyers, R. E., and Cantley, L. C. Phosphoinositide kinases. Annu.Rev.Biochem. 67 (1998) 481-507.

[2]. Vanhaesebroeck, B., Leevers, S. J., Ahmadi, K., Timms, J., Katso, R., Driscoll, P. C., Woscholski, R., Parker, P. J., and Waterfield, M. D. Synthesis and function of 3-phosphorylated inositol lipids. Annu.Rev.Biochem. 70 (2001) 535-602.

[3]. Odorizzi, G., Babst, M., and Emr, S. D. Phosphoinositide signaling and the regulation of membrane trafficking in yeast. Trends Biochem.Sci. 25 (2000) 229-235.

[4]. Schu, P. V., Takegawa, K., Fry, M. J., Stack, J. H., Waterfield, M. D., and Emr, S. D. Phosphatidylinositol 3-kinase encoded by yeast VPS34 gene essential for protein sorting. Science 260 (1993) 88-91.

[5]. Herman, P. K., Stack, J. H., and Emr, S. D. An essential role for a protein and lipid kinase complex in secretory protein sorting. Trends Cell Biol. 2 (1992) 363-368.

[6]. Kihara, A., Noda, T., Ishihara, N., and Ohsumi, Y. Two distinct Vps34 phosphatidylinositol 3-kinase complexes function in autophagy and carboxypeptidase Y sorting in Saccharomyces cerevisiae. J.Cell Biol. 152 (2001) 519-530.

[7]. Wurmser, A. E. and Emr, S. D. Novel PtdIns(3)P-binding protein Etf1 functions as an effector of the Vps34 PtdIns 3-kinase in autophagy. J.Cell Biol. 158 (2002) 761-772.

[8]. Stack, J. H., DeWald, D. B., Takegawa, K., and Emr, S. D. Vesicle-mediated protein transport: regulatory interactions between the Vps15 protein kinase and the Vps34 PtdIns 3-kinase essential for protein sorting to the vacuole in yeast. J.Cell Biol. 129 (1995) 321-334.

[9]. Panaretou, C., Domin, J., Cockcroft, S., and Waterfield, M. D. Characterization of p150, an adaptor protein for the human phosphatidylinositol (PtdIns) 3-kinase. Substrate presentation by phosphatidylinositol transfer protein to the p150.Ptdins 3-kinase complex. J.Biol.Chem. 272 (1997) 2477-2485.

[10]. Corvera, S. Phosphatidylinositol 3-kinase and the control of endosome dynamics: New players defined by structural motifs. Traffic 2 (2001) 859-866.

[11]. Simonsen, A., Wurmser, A. E., Emr, S. D., and Stenmark, H. The role of phosphoinositides in membrane transport. Curr.Opin.Cell Biol. 13 (2001) 485-492.

[12]. Song, X., Xu, W., Zhang, A., Huang, G., Liang, X., Virbasius, J. V., Czech, M. P., and Zhou, G. W. Phox homology domains specifically bind phosphatidylinositol phosphates. Biochemistry 40 (2001) 8940-8944.

[13]. Cheever, M. L., Sato, T. K., de Beer, T., Kutateladze, T. G., Emr, S. D., and Overduin, M. Phox domain interaction with PtdIns(3)P targets the Vam7 t-SNARE to vacuole membranes. Nat.Cell Biol. 3 (2001) 613-618.

[14]. Kanai, F., Liu, H., Field, S. J., Akbary, H., Matsuo, T., Brown, G. E., Cantley, L. C., and Yaffe, M. B. The PX domains of p47phox and p40phox bind to lipid products of PI(3)K. Nat.Cell Biol. 3 (2001) 675-678.

[15]. Xu, Y., Hortsman, H., Seet, L., Wong, S. H., and Hong, W. SNX3 regulates endosomal function through its PX-domain-mediated interaction with PtdIns(3)P. Nat.Cell Biol. 3 (2001) 658-666.

[16]. Corvera, S., D'Arrigo, A., and Stenmark, H. Phosphoinositides in membrane traffic. Curr.Opin.Cell Biol. 11 (1999) 460-465.

[17]. Fruman, D. A., Rameh, L. E., and Cantley, L. C. Phosphoinositide binding domains: embracing 3-phosphate. Cell 97 (1999) 817-820.

[18]. Wurmser, A. E., Gary, J. D., and Emr, S. D. Phosphoinositide 3-kinases and their FYVE domain-containing effectors as regulators of vacuolar/lysosomal membrane trafficking pathways. J.Biol.Chem. 274 (1999) 9129-9132.

[19]. Nielsen, E., Christoforidis, S., Uttenweiler-Joseph, S., Miaczynska, M., Dewitte, F., Wilm, M., Hoflack, B., and Zerial, M. Rabenosyn-5, a novel Rab5 effector, is complexed with hVPS45 and recruited to endosomes through a FYVE finger domain. J.Cell Biol. 151 (2000) 601-612.

[20]. Simonsen, A., Lippe, R., Christoforidis, S., Gaullier, J. M., Brech, A., Callaghan, J., Toh, B. H., Murphy, C., Zerial, M., and Stenmark, H. EEA1 links PI(3)K function to Rab5 regulation of endosome fusion. Nature 394 (1998) 494-498.

[21]. Cormont, M., Mari, M., Galmiche, A., Hofman, P., and Marchand-Brustel, Y. A FYVE-finger-containing protein, Rabip4, is a Rab4 effector involved in early endosomal traffic. Proc.Natl.Acad.Sci.U.S.A 98 (2001) 1637-1642.

[22]. Kauppi, M., Simonsen, A., Bremnes, B., Vieira, A., Callaghan, J., Stenmark, H., and Olkkonen, V. M. The small GTPase Rab22 interacts with EEA1 and controls endosomal membrane trafficking. J.Cell Sci. 115 (2002) 899-911.

[23]. Murray, J. T., Panaretou, C., Stenmark, H., Miaczynska, M., and Backer, J. M. Role of Rab5 in the recruitment of hVps34/p150 to the early endosome. Traffic 3 (2002) 416-427.

[24]. Stein, M. P., Feng, Y., Cooper, K. L., Welford, A. M., and Wandinger-Ness, A. Human VPS34 and p150 are Rab7 interacting partners. Traffic 4 (2003) 754-771.

[25]. Davidson, H. W. Wortmannin causes mistargeting of procathepsin D. Evidence for the involvement of a phosphatidylinositol 3-kinase in vesicular transport to lysosomes. J.Cell Biol. 130 (1995) 797-805.

[26]. Brown, W. J., DeWald, D. B., Emr, S. D., Plutner, H., and Balch, W. E. Role for phosphatidylinositol 3-kinase in the sorting and transport of newly synthesized lysosomal enzymes in mammalian cells. J.Cell Biol. 130 (1995) 781-796.

[27]. Row, P. E., Reaves, B. J., Domin, J., Luzio, J. P., and Davidson, H. W. Overexpression of a rat kinase-deficient phosphoinositide 3-kinase, Vps34p, inhibits cathepsin D maturation. Biochem J. 353 (2001) 655-661.

[28]. Siddhanta, U., McIlroy, J., Shah, A., Zhang, Y., and Backer, J. M.. Distinct roles for the p110alpha and hVPS34 phosphatidylinositol 3'- kinases in vesicular trafficking, regulation of the actin cytoskeleton, and mitogenesis. J.Cell Biol. 143 (1998) 1647-1659.

[29]. Futter, C. E., Collinson, L. M., Backer, J. M., and Hopkins, C. R. Human VPS34 is required for internal vesicle formation within multivesicular endosomes. J.Cell Biol. 155 (2001) 1251-1264.

[30]. Gruenberg, J. and Maxfield, F. R. Membrane transport in the endocytic pathway. Curr.Opin.Cell Biol. 7 (1995) 552-563.

[31]. Petiot, A., Ogier-Denis, E., Blommaart, E. F., Meijer, A. J., and Codogno, P. Distinct classes of phosphatidylinositol 3'-kinases are involved in signaling pathways that control macroautophagy in HT-29 cells. J.Biol.Chem. 275 (2000) 992-998.

[32]. Meyers, R. and Cantley, L. C. Cloning and characterization of a wortmannin-sensitive human phosphatidylinositol 4-kinase. J.Biol.Chem. 272 (1997) 4384-4390.

[33]. Sui, G., Soohoo, C., Affar, e. B., Gay, F., Shi, Y., Forrester, W. C., and Shi, Y. A DNA vector-based RNAi technology to suppress gene expression in mammalian cells. Proc.Natl.Acad.Sci.U.S.A 99 (2002) 5515-5520.

[34]. Paul, C. P., Good, P. D., Winer, I., and Engelke, D. R. Effective expression of small interfering RNA in human cells. Nat.Biotechnol. 20 (2002) 505-508.

[35]. Brummelkamp, T. R., Bernards, R., and Agami, R. A system for stable expression of short interfering RNAs in mammalian cells. Science 296 (2002) 550-553.

[36]. Ory, D. S., Neugeboren, B. A., and Mulligan, R. C. A stable human-derived packaging cell line for production of high titer retrovirus/vesicular stomatitis virus G pseudotypes. Proc.Natl.Acad.Sci U.S.A 93 (1996) 11400-11406.

[37]. Wilson, A. L., Erdman, R. A., and Maltese, W. A. Association of Rab1B with GDP-dissociation inhibitor (GDI) is required for recycling but not initial membrane targeting of the Rab protein. J.Biol.Chem. 271 (1996) 10932-10940.

[38]. Maltese, W. A., Reitz, B. A., and Volpe, J. J. Effects of isoleucine deprivation on synthesis of sterols and fatty acids in LM-cells. J.Biol.Chem. 256 (1981) 2185-2193.

[39]. Dugan, J. M., deWit, C., McConlogue, L., and Maltese, W. A. The ras-related GTP binding protein, Rab1B, regulates early steps in exocytic transport and processing of β-amyloid precursor protein. J.Biol.Chem. 270 (1995) 10982-10989.

[40]. Wilson, A. L., Erdman, R. A., Castellano, F., and Maltese, W. A. Prenylation of Rab8 GTPase by type I and type II geranylgeranyl transferases. Biochem.J. 333 (1998) 497-504.

[41]. Kihara, A., Kabeya, Y., Ohsumi, Y., and Yoshimori, T. Beclin-phosphatidylinositol 3-kinase complex functions at the trans- Golgi network. EMBO Rep. 2 (2001) 330-335.

[42]. Kuronita, T., Eskelinen, E. L., Fujita, H., Saftig, P., Himeno, M., and Tanaka, Y. A role for the lysosomal membrane protein LGP85 in the biogenesis and maintenance of endosomal and lysosomal morphology. J.Cell Sci. 115 (2002) 4117-4131.

[43]. Kobayashi, T., Stang, E., Fang, K. S., de Moerloose, P., Parton, R. G., and Gruenberg, J. A lipid associated with the antiphospholipid syndrome regulates endosome structure and function. Nature 392 (1998) 193-197.

[44]. Le Borgne, R. and Hoflack, B. Protein transport from the secretory to the endocytic pathway in mammalian cells. Biochim.Biophys.Acta 1404 (1998) 195-209.

[45]. Ghosh, P., Dahms, N. M., and Kornfeld, S. Mannose 6-phosphate receptors: new twists in the tale. Nat.Rev.Mol.Cell Biol. 4 (2003) 202-212.

[46]. Press, B., Feng, Y., Hoflack, B., and Wandinger-Ness, A. Mutant Rab7 causes the accumulation of cathepsin D and cation-independent mannose 6-phosphate receptor in an early endocytic compartment. J.Cell Biol. 140 (1998) 1075-1089.

[47]. Hirst, J., Futter, C. E., and Hopkins, C. R. The kinetics of mannose 6-phosphate receptor trafficking in the endocytic pathway in HEp-2 cells: the receptor enters and rapidly leaves multivesicular endosomes without accumulating in a prelysosomal compartment. Mol.Biol.Cell 9 (1998) 809-816.

[48]. Traganos, F. and Darzynkiewicz, Z. Lysosomal proton pump activity: supravital cell staining with acridine orange differentiates leukocyte subpopulations. Methods Cell Biol. 41 (1994) 185-194.

[49]. Paglin, S., Hollister, T., Delohery, T., Hackett, N., McMahill, M., Sphicas, E., Domingo, D., and Yahalom, J. A novel response of cancer cells to radiation involves autophagy and formation of acidic vesicles. Cancer Res 61 (2001) 439-444.

[50]. Kanzawa, T., Kondo, Y., Ito, H., Kondo, S., and Germano, I. Induction of autophagic cell death in malignant glioma cells by arsenic trioxide. Cancer Res. 63 (2003) 2103-2108.

[51]. Gough, N. R., Zweifel, M. E., Martinez-Augustin, O., Aguilar, R. C., Bonifacino, J. S., and Fambrough, D. M. Utilization of the indirect lysosome targeting pathway by lysosome-associated membrane proteins (LAMPs) is influenced largely by the C-terminal residue of their GYXXphi targeting signals. J.Cell Sci. 112 (1999) 4257-4269.

[52]. Christoforidis, S., McBride, H. M., Burgoyne, R. D., and Zerial, M. The Rab5 effector EEA1 is a core component of endosome docking. Nature 397 (1999) 621-625.

[53]. Petiot, A., Faure, J., Stenmark, H., and Gruenberg, J. PI3P signaling regulates receptor sorting but not transport in the endosomal pathway. J. Cell Biol. 162 (2003) 971-979.

[54]. Li, G. and Stahl, P. D. Structure-function relationship of the small GTPase rab5. J.Biol.Chem. 268 (1993) 24475-24480.

[55]. Mayran, N., Parton, R. G., and Gruenberg, J. Annexin II regulates multivesicular endosome biogenesis in the degradation pathway of animal cells. EMBO J. 22 (2003) 3242-3253.

[56]. Katzmann, D. J., Odorizzi, G., and Emr, S. D. Receptor downregulation and multivesicular-body sorting. Nat.Rev.Mol.Cell Biol. 3 (2002) 893-905.

[57]. Pohlmann, R., Boeker, M. W., and von Figura, K. The two mannose 6-phosphate receptors transport distinct complements of lysosomal proteins. J.Biol.Chem. 270 (1995) 27311-27318.

[58]. Rijnboutt, S., Stoorvogel, W., Geuze, H. J., and Strous, G. J. Identification of subcellular compartments involved in biosynthetic processing of cathepsin D. J.Biol.Chem. 267 (1992) 15665-15672.

[59]. Delbruck, R., Desel, C., von Figura, K., and Hille-Rehfeld, A. Proteolytic processing of cathepsin D in prelysosomal organelles. Eur.J.Cell Biol. 64 (1994) 7-14.

[60]. Hentze, M., Hasilik, A., and von Figura, K. Enhanced degradation of cathepsin D synthesized in the presence of the threonine analog beta-hydroxynorvaline. Arch.Biochem.Biophys. 230 (1984) 375-382.

[61]. Reilly, J. J., Jr., Mason, R. W., Chen, P., Joseph, L. J., Sukhatme, V. P., Yee, R., and Chapman, H. A., Jr. Synthesis and processing of cathepsin L, an elastase, by human alveolar macrophages. Biochem.J 257 (1989) 493-498.

[62]. Nissler, K., Strubel, W., Kreusch, S., Rommerskirch, W., Weber, E., and Wiederanders, B. The half-life of human procathepsin S. Eur.J Biochem. 263 (1999) 717-725.

[63]. Jones, S. M., Alb, J. G., Jr., Phillips, S. E., Bankaitis, V. A., and Howell, K. E. A phosphatidylinositol 3-kinase and phosphatidylinositol transfer protein act synergistically in formation of constitutive transport vesicles from the trans-Golgi network. J Biol.Chem. 273 (1998) 10349-10354.

[64]. Hickinson, D. M., Lucocq, J. M., Towler, M. C., Clough, S., James, J., James, S. R., Downes, C. P., and Ponnambalam, S. Association of a phosphatidylinositol-specific 3-kinase with a human trans-Golgi network resident protein. Curr.Biol. 7 (1997) 987-990.

[65]. Gillooly, D. J., Raiborg, C., and Stenmark, H. Phosphatidylinositol 3-phosphate is found in microdomains of early endosomes. Histochem.Cell Biol. 120 (2003) 445-453.

[66]. Gillooly, D. J., Morrow, I. C., Lindsay, M., Gould, R., Bryant, N. J., Gaullier, J. M., Parton, R. G., and Stenmark, H. Localization of phosphatidylinositol 3-phosphate in yeast and mammalian cells. EMBO J. 19 (2000) 4577-4588.

[67]. Leevers, S. J., Vanhaesebroeck, B., and Waterfield, M. D. Signalling through phosphoinositide 3-kinases: the lipids take centre stage. Curr.Opin.Cell Biol. 11 (1999) 219-225.

[68]. Prior, I. A. and Clague, M. J. Localization of a class II phosphatidylinositol 3-kinase, PI3KC2alpha, to clathrin-coated vesicles. Mol.Cell Biol.Res Commun. 1 (1999) 162-166.

[69]. Arcaro, A., Volinia, S., Zvelebil, M. J., Stein, R., Watton, S. J., Layton, M. J., Gout, I., Ahmadi, K., Downward, J., and Waterfield, M. D. Human phosphoinositide 3-kinase C2beta, the role of calcium and the C2 domain in enzyme activity. J.Biol.Chem. 273 (1998) 33082-33090.

[70]. Kisseleva, M. V., Wilson, M. P., and Majerus, P. W. The isolation and characterization of a cDNA encoding phospholipid-specific inositol polyphosphate 5-phosphatase. J Biol.Chem. 275 (2000) 20110-20116.

[71]. Norris, F. A., Auethavekiat, V., and Majerus, P. W. The isolation and characterization of cDNA encoding human and rat brain inositol polyphosphate 4-phosphatase. J Biol.Chem. 270 (1995) 16128-16133.

[72]. Norris, F. A., Atkins, R. C., and Majerus, P. W. The cDNA cloning and characterization of inositol polyphosphate 4-phosphatase type II. Evidence for conserved alternative splicing in the 4-phosphatase family. J Biol.Chem. 272 (1997) 23859-23864.

[73]. Naga Prasad, S. V., Laporte, S. A., Chamberlain, D., Caron, M. G., Barak, L., and Rockman, H. A. Phosphoinositide 3-kinase regulates β2-adrenergic receptor endocytosis by AP-2 recruitment to the receptor/ β-arrestin complex. J. Cell Biol. 158 (2002) 563-575.

[74]. Futter, C. E., Pearse, A., Hewlett, L. J., and Hopkins, C. R. Multivesicular endosomes containing internalized EGF-EGF receptor complexes mature and then fuse directly with lysosomes. J.Cell Biol. 132 (1996) 1011-1023.

[75]. Haj, F. G., Verveer, P. J., Squire, A., Neel, B. G., and Bastiaens, P. I. H. Imaging sites of receptor dephosphorylation by PTP1B on the surface of the endoplasmic reticulum. Science 295 (2002) 1708-1711.

[76]. Gill, G. N. A pit stop at the ER. Science 295 (2002) 1654-1655.

[77]. Burke, P., Schooler, K., and Wiley, H. S. Regulation of epidermal growth factor receptor signaling by endocytosis and intracellular trafficking. Mol.Biol.Cell 12 (2001) 1897-1910.

[78]. Wiley, H. S. and Burke, P. M. Regulation of receptor tyrosine kinase signaling by endocytic trafficking. Traffic 2 (2001) 12-18.

[79]. Babst, M., Wendland, B., Estepa, E. J., and Emr, S. D. The Vps4p AAA ATPase regulates membrane association of a Vps protein complex required for normal endosome function. EMBO J. 17 (1998) 2982-2993.

[80]. Bishop, N. and Woodman, P. ATPase-defective mammalian VPS4 localizes to aberrant endosomes and impairs cholesterol trafficking. Mol.Biol.Cell 11 (2000) 227-239.

[81]. Whitley, P., Reaves, B. J., Hashimoto, M., Riley, A. M., Potter, B. V., and Holman, G. D. Identification of mammalian Vps24p as an effector of phosphatidylinositol 3,5-bisphosphate-dependent endosome compartmentalization. J.Biol.Chem. 278 (2003) 38786-38795.

[82]. Sbrissa, D., Ikonomov, O. C., and Shisheva, A. PIKfyve, a mammalian ortholog of yeast Fab1p lipid kinase, synthesizes 5-phosphoinositides. Effect of insulin. J.Biol.Chem. 274 (1999) 21589-21597.

[83]. Ikonomov, O. C., Sbrissa, D., Foti, M., Carpentier, J. L., and Shisheva, A. PIKfyve controls fluid phase endocytosis but not recycling/degradation of endocytosed receptors or sorting of procathepsin D by regulating multivesicular body morphogenesis. Mol.Biol.Cell 14 (2003) 4581-4591.

[84]. Drobak, B. K., Watkins, P. A., Bunney, T. D., Dove, S. K., Shaw, P. J., White, I. R., and Millner, P. A. Association of multiple GTP-binding proteins with the plant cytoskeleton and nuclear matrix. Biochem.Biophys.Res Commun. 210 (1995) 7-13.

[85]. Bunney, T. D., Watkins, P. A., Beven, A. F., Shaw, P. J., Hernandez, L. E., Lomonossoff, G. P., Shanks, M., Peart, J., and Drobak, B. K. Association of phosphatidylinositol 3-kinase with nuclear transcription sites in higher plants. Plant Cell 12 (2000) 1679-1688.

Figure Legends

Fig 1. siRNA-mediated suppression of hVps34 expression in U-251 glioma cells. (A) U-251 cells infected with retrovirus carrying the control or hVps34 KD siRNA sequences surviving after 5 days of puromycin selection were subjected to immunoblot analysis with a polyclonal anti-hVps34 IgG as described in the Methods. Nuclear lamin B_2 served as a loading control. (B) Phase contrast image of the live control and KD cells. The scale bar equals 10 μm.

Fig 2. Vacuoles in the hVps34 KD cells are membrane-bound structures with occasional internal vesicles and electron dense material. Control and hVps34 KD cells were examined by electron microscopy. (A) Control and KD cells magnified 3,900X. Bar represents 5 μm. (B) Highlighted region of KD cell from panel A at 21,000X. The bar represents 1 μm. Labeled structures: mitochondria (m), nucleus (n), vacuole (v). The arrowhead points to single membrane surrounding the vacuole. Arrows point to occasional internal vesicles and electron dense material.

Fig. 3. Vacuoles in the hVps34 KD cells exhibit characteristics of late endosomes or lysosomes. Control and hVps34 KD cells were seeded at 100,000 cells/dish in 35 mm dishes. 24 h later cells were examined by immunofluorescence microscopy using the primary antibodies indicated at the left of the figure. The bar represents 10 μm.

Fig. 4. Vacuoles in the hVps34 KD cells are acidic and receive traffic from the endocytic compartment. (A) Control and hVps34 KD cells were incubated with 2.5 μg/ml acridine orange for 30 min. Live cells were then examined by fluorescence microscopy using green (excitation

wavelength: 500 nm, emission wavelength: 520 nm) and red (excitation wavelength: 488 nm, emission wavelength 655 nm) filters. Red fluorescence emanates from AO in acidic compartments. The scale bar represents 10 μm. (B) Control and KD cells were incubated with 500 μg/ml TxR-dextran for 16 h. Following a 2 h incubation, cells were fixed and co-stained with a monoclonal antibody against LAMP1. Arrows indicate vacuoles containing both LAMP1 and TxR-dextran. Arroheads point to vacuoles lacking TxR-dextran. The bar represents 10 μm.

Fig. 5. Suppression of hVps34 expression does not prevent membrane association of the early endosome marker, EEA1. (A) Control and hVps34 KD cells were seeded at 100,000 cells/dish in 35 mm dishes. 24 h later cells were examined by immunofluorescence microscopy using an anti-EEA1 antibody. Control cells treated with 1 μM wortmannin for 1 h served as a positive control for release of EEA1. (B) Cytosolic (S100) and particulate (P100) fractions prepared from control and KD cells as described in the Methods were subjected to immunoblot analysis with an antibody against EEA1. Control cells treated with 1 μM wortmannin for 1 h served as a positive control. The percentage of EEA1 in each fraction was determined using a Kodak 440CF Image Station. Similar results were obtained in two separate experiments.

Fig. 6. Suppression of hVps34 expression does not interfere with the endocytosis of a fluid phase marker, horseradish peroxidase (HRP). (A) Control (-▲-) and hVps34 KD (-■-) cells were incubated for the indicated periods of time with 2 mg/ml HRP in DMEM + 1% BSA. Washed cells were lysed and HRP activity was determined as described in the Methods. Each point represents the mean ± S.E. from triplicate dishes of each cell line.

Fig. 7. Suppression of hVps34 expression potentiates EGFR signaling but does not impede receptor degradation. Control and hVps34 KD cells were stimulated with EGF after overnight incubation with

serum-free medium. (A) Cells were fixed and co-stained with EGFR and LGP85 antibodies at 30 min or 60 min after addition of EGF. Arrows indicate vacuoles positive for both the EGFR and LGP85. The scale bar represents 10 μm. For EGFR degradation, phosphorylation, and signaling, the control and KD cells were harvested at the indicated times after the addition of EGF and subjected to immunoblot analysis for (B) total EGFR, (C) phospho-EGFR, and (D) phospho-ERK1/2 and total ERK1/2. The bar graphs illustrate the data generated from Kodak Imager scans of blots from triplicate cultures of each cell line.

Fig. 8. The late endosomal intermediate form of cathepsin D accumulates in the absence of hVps34, but there is no inhibition of procathepsin D processing. (A) Control and hVps34 KD cells were seeded at 100,000 cells/dish in 35 mm dishes. Cells were labeled with 100 μCi/ml ^{35}S-methionine, then harvested after 30 min or chased in medium with unlabeled methionine for 4 h. A separate control culture was incubated with 15 mM NH_4Cl duing the 4 h chase. Cathepsin D was immunoprecipitated and subjected to SDS-PAGE and fluorography. (B) Immunoblot analysis of endogenous cathepsin D in whole cell lysates from control and KD cells.

Fig. 9. Swollen late endosomes in hVps34KD cells can fuse with lysosomes. (A) hVps34 KD cells were stained for endogenous peroxidase activity with DAB and then examined using electron microscopy. The arrow indicates a point of contact between smaller DAB-positive lysosome and a larger DAB-negative vacuole. The arrowheads indicate remnants of lysosomes that appear to have merged with the vacuoles. The bar represents 1 μm. (B) The KD cells were subjected to immunogold labeling with an antibody against cathepsin D. The left panel depicts a lysosome heavily labeled for cathepsin D (arrow) adjacent to a larger electron lucent vacuole. The right panel shows cathepsin D delivered to the lumen of an enlarged vacuole (arrowhead). The bar represents 0.5 μm.

Fig. 10. hVps34 KD cells exhibit a marked reduction in growth rate. (A) Following 2 days of selection, control (-▲-) and hVps34 KD (-■-) cells were seeded in 35 mm dishes at an equal density of 50,000 cells/dish. At the indicated time points, triplicate dishes from each cell line were harvested and counted with a Coulter Z1 particle counter (mean ± S.E.) (B) control (■) and KD (■) cells were seeded in 25 cm^2 flasks at 150,000 cells/flask. On the indicated days triplicate flasks of each cell line were incubated with ^{3}H-thymidine (1.0 μCi/ml) for 5 h. Radioactivity incorporated into TCA-precipitable material was counted and normalized to total cellular protein (mean ± S.E.). (C) Control (■) and KD (■) cells were seeded in 60 mm dishes at 200,000 cells/dish. On the indicated days, duplicate dishes from each cell line were harvested and stained with annexin-V. Annexin-positive cells were counted using a Guava personal cytometer. Cells treated overnight with TNFα (□) served as a positive control for apoptosis.

Fig.1

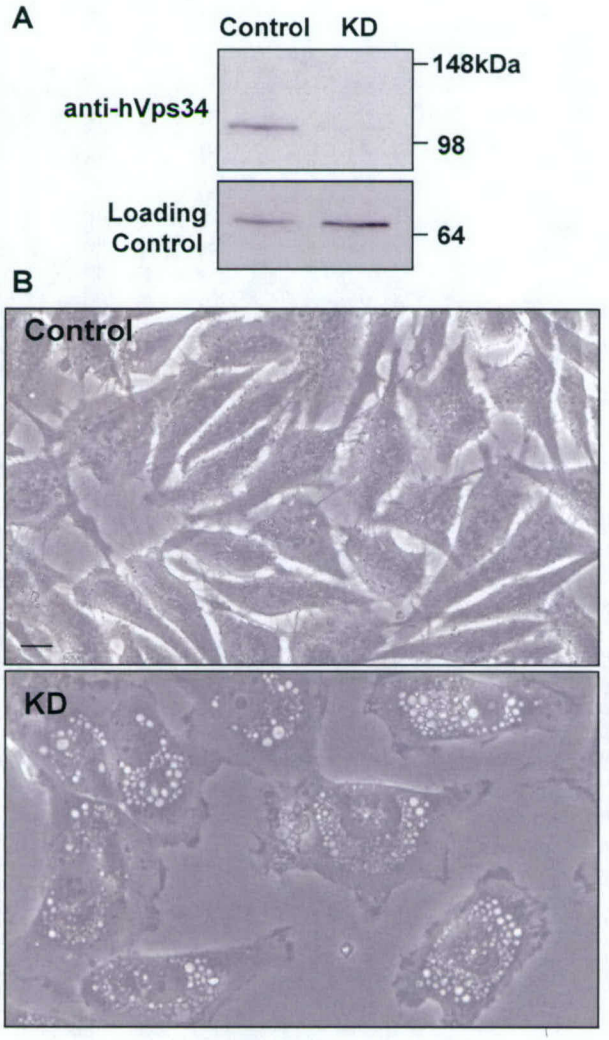
A
Control
KD
148kDa
anti-hVps34
98
Loading
Control
64
B
Control
KD

Fig. 2

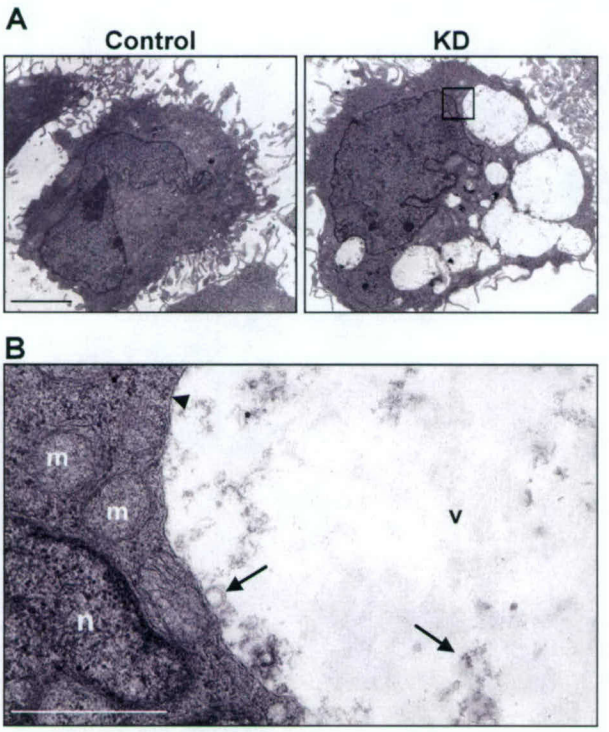

Fig. 3

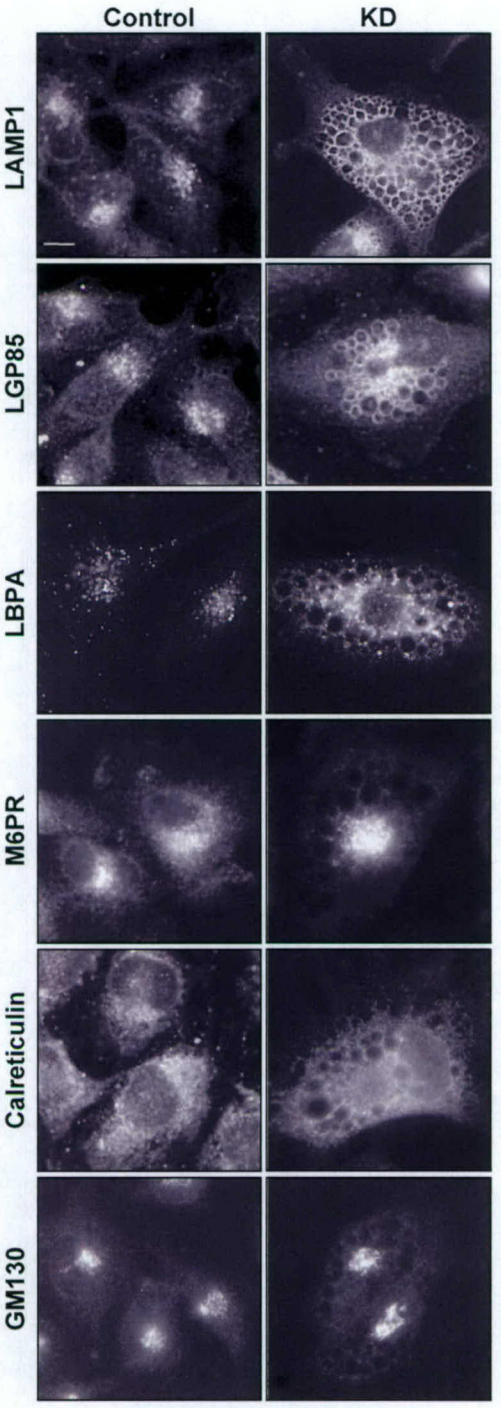

Fig. 4

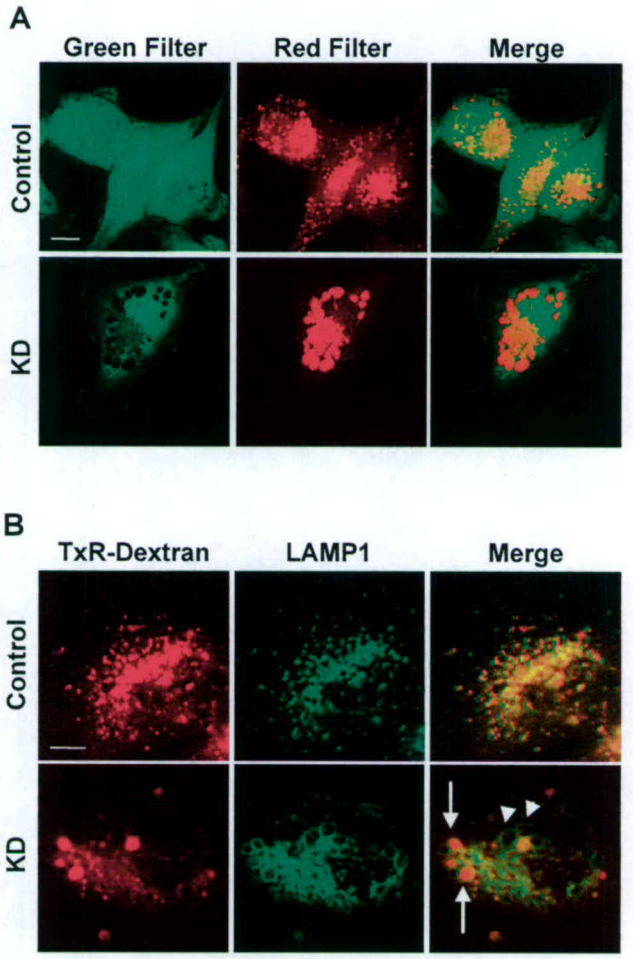
A
Green Filter
Red Filter
Merge
Control
KD
B
TxR-Dextran
LAMP1
Merge
Control
KD

Fig. 5

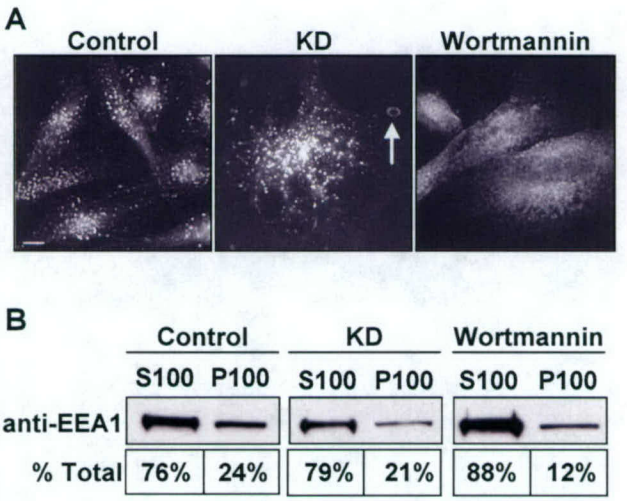
A
Control
KD
Wortmannin
B
Control
KD
Wortmannin
S100
P100
S100
P100
S100
P100
anti-EEA1
% Total
76%
24%
79%
21%
88%
12%

Fig. 6

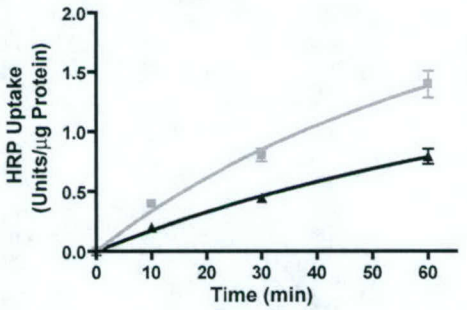
HRP Uptake
(Units/µg Protein)
2.0
1.5
1.0
0.5
0.0
0
10
20
30
40
50
60
Time (min)

Fig. 7

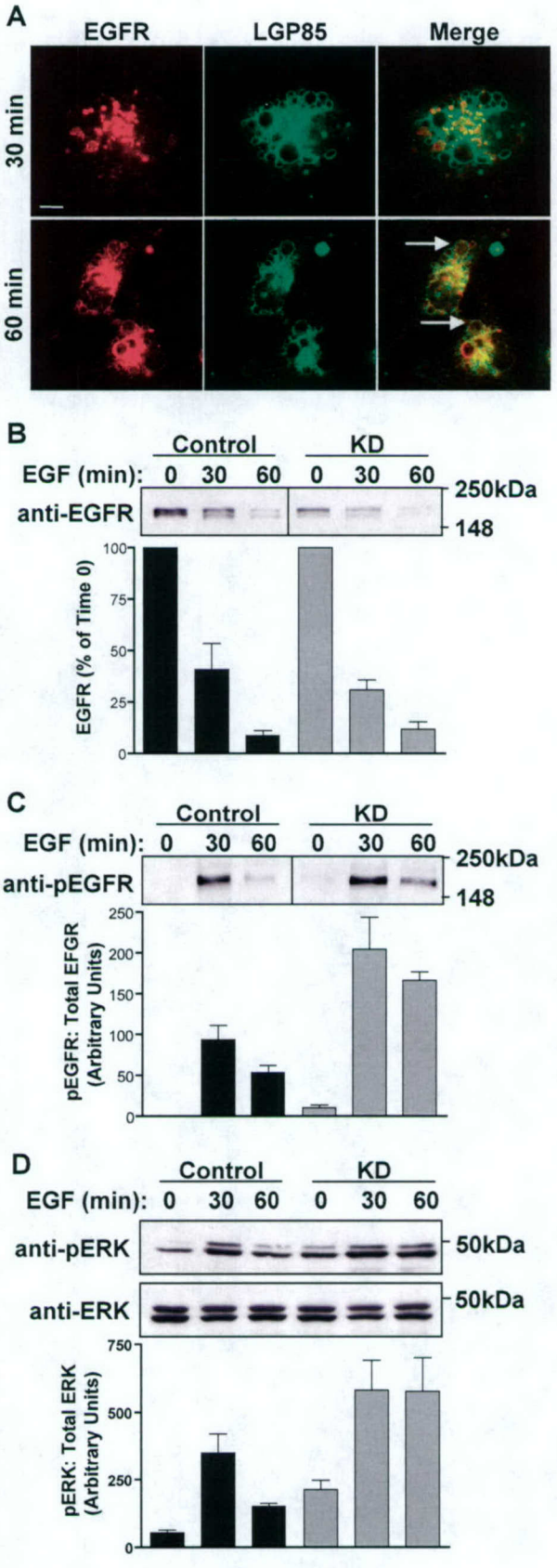
A
EGFR
LGP85
Merge
30 min
60 min
B
Control
KD
EGF (min): 0 30 60 0 30 60
anti-EGFR
250kDa
148
EGFR (% of Time 0)
100
75
50
25
0
C
Control
KD
EGF (min): 0 30 60 0 30 60
anti-pEGFR
250kDa
148
pEGFR: Total EFGR (Arbitrary Units)
250
200
150
100
50
0
D
Control
KD
EGF (min): 0 30 60 0 30 60
anti-pERK
50kDa
anti-ERK
50kDa
pERK: Total ERK (Arbitrary Units)
750
500
250
0

Fig. 8

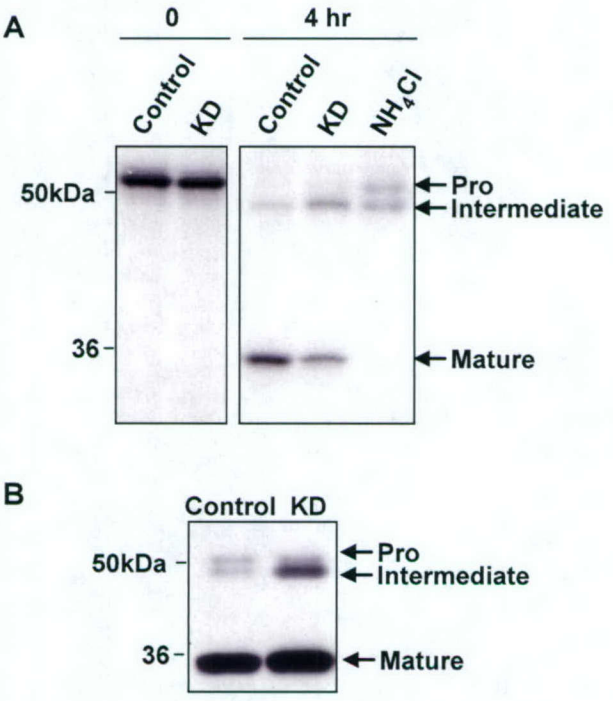
A
0
4 hr
Control
KD
Control
KD
NH4Cl
50kDa
36
Pro
Intermediate
Mature
B
Control KD
50kDa
36
Pro
Intermediate
Mature

Fig. 9

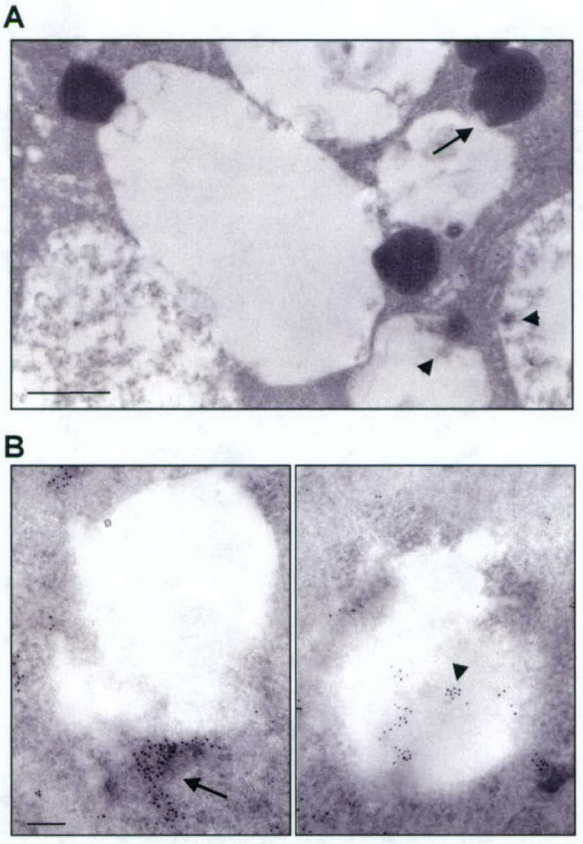

Fig. 10

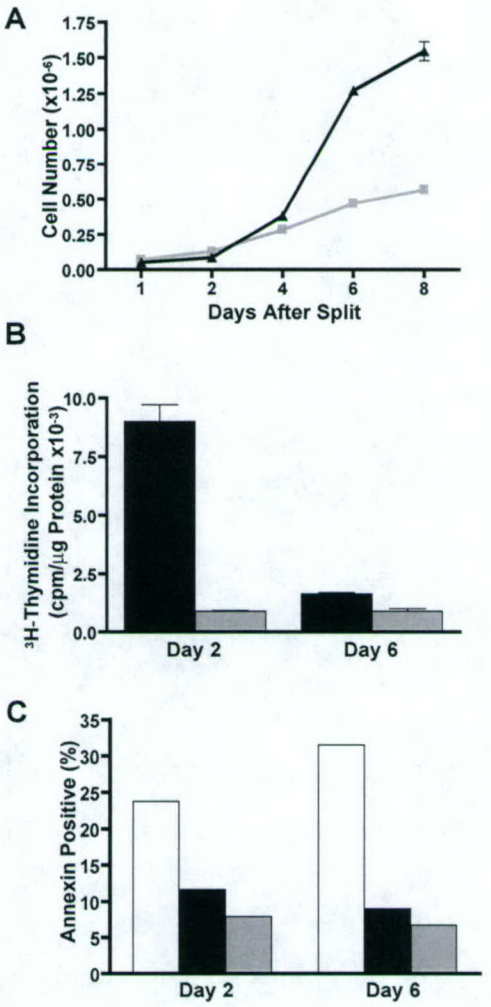
A
Cell Number (x10⁻⁶)
1.75
1.50
1.25
1.00
0.75
0.50
0.25
0.00
1
2
4
6
8
Days After Split
B
³H-Thymidine Incorporation (cpm/μg Protein x10⁻³)
10.0
7.5
5.0
2.5
0.0
Day 2
Day 6
C
Annexin Positive (%)
35
30
25
20
15
10
5
0
Day 2
Day 6